MICROCOPY RESOLUTION TEST CHART
NATIONAL BUREAU OF STANDARDS-1963-A

AFGL-TR-83-0195

THE FEASIBILITY OF USING PRECURSOR AEROSOL PARAMETERS
TO PREDICT VISIBILITY IN FOG AND HAZE

J.T. Hanley
E.J. Mack
B.J. Wattle
J.N. Kile

Calspan Corporation
P.O. Box 400
Buffalo, New York 14225

Final Report
2 February 1982 - 15 July 1983

July 1983

DTIC
ELECTE
JAN 2 4 1984
S
E

AD A137141

DTIC FILE COPY

84 01 23 035

This report has been reviewed by the ESD Public Affairs Office (PA) and is releasable to the National Technical Information Service (NTIS).

This technical report has been reviewed and is approved for publication

BRUCE A. KUNKEL
Contract Monitor

DONALD D. GRANTHAM
Chief, Tropospheric Structure Branch

FOR THE COMMANDER

ROBERT A. McCLATCHEY
Director, Meteorology Division

REPORT DOCUMENTATION PAGE	READ INSTRUCTIONS BEFORE COMPLETING FORM

1. REPORT NUMBER AFGL-TR-83-0195	2. GOVT ACCESSION NO. A157141	3. RECIPIENT'S CATALOG NUMBER

4. TITLE *(and Subtitle)* The Feasibility of Using Precursor Aerosol Parameters to Predict Visibility in Fog and Haze	5. TYPE OF REPORT & PERIOD COVERED Final Report 2 Feb. '82-15 July '83
	6. PERFORMING ORG. REPORT NUMBER 7028-M-1

7. AUTHOR(s) J. T. Hanley, E. J. Mack, B. J. Wattle and J. N. Kile	8. CONTRACT OR GRANT NUMBER(s) F19628-82-C-0034

9. PERFORMING ORGANIZATION NAME AND ADDRESS Calspan Corporation P. O. Box 400 Buffalo, N.Y. 14225	10. PROGRAM ELEMENT, PROJECT, TASK AREA & WORK UNIT NUMBERS 62101F 667014AC

11. CONTROLLING OFFICE NAME AND ADDRESS Air Force Geophysics Laboratory Hanscom Air Force Base, Massachusetts 01731 Monitor/Bruce Kunkel/LYT	12. REPORT DATE July 1983
	13. NUMBER OF PAGES 68

14. MONITORING AGENCY NAME & ADDRESS*(if different from Controlling Office)*	15. SECURITY CLASS. *(of this report)* Unclassified
	15a. DECLASSIFICATION/DOWNGRADING SCHEDULE

16. DISTRIBUTION STATEMENT *(of this Report)*

Approved for public release; distribution unlimited.

17. DISTRIBUTION STATEMENT *(of the abstract entered in Block 20, if different from Report)*

18. SUPPLEMENTARY NOTES

19. KEY WORDS *(Continue on reverse side if necessary and identify by block number)*

Precursor Aerosol	Fog Visibility	Haze
Visibility Prediction	Visibility Forecast	
Haze Visibility	Fog	

20. ABSTRACT *(Continue on reverse side if necessary and identify by block number)*

Calspan Corporation, in collaboration with the Air Force Geophysics Laboratory (AFGL), examined the feasibility of predicting the visibility in fog and haze based on precursor aerosol characteristics. A field study to gather pertinent data was conducted jointly by AFGL and Calspan personnel in the vicinity of Cape Cod during June 1982. Measurements were made at two AFGL-operated measurement sites: the AFGL Weather Test Facility at Otis AFB and a remote coastal site at the Nobska Lighthouse, Woods

DD _{1 JAN 73} FORM 1473   EDITION OF 1 NOV 65 IS OBSOLETE

20. ABSTRACT (Continued)

Hole. Precursor aerosol measurements including particle and CCN concentrations, aerosol mass loading, chemical composition and ambient visibility were obtained on a daily basis for correlation with the visibility measured in subsequent fogs or hazes associated with increasing ambient humidity. Additionally, the differences between the aerosol characteristics measured at the coastal and inland sites were investigated, and the utility of using the general wind field pattern to infer air mass aerosol characteristics was assessed.

Accession For	
NTIS GRA&I	☒
DTIC TAB	☐
Unannounced	☐
Justification	
By	
Distribution/	
Availability Codes	
Dist	Avail and/or Special
A-1	

TABLE OF CONTENTS

Section 1
INTRODUCTION AND SUMMARY

1.1 INTRODUCTION

Under Contract No. F19628-82-C-0034, Calspan Corporation collaborated with the Air Force Geophysics Laboratory (AFGL) in an investigation to examine the feasibility of predicting the visibility in fog and haze based on precursor aerosol characteristics. A field study to gather pertinent data was conducted jointly by AFGL and Calspan personnel in the vicinity of Cape Cod during June 1982. Measurements were made at two AFGL-operated measurement sites: the AFGL Weather Test Facility at Otis AFB and a remote coastal site at the Nobska Lighthouse, Woods Hole. Precursor aerosol measurements including particle and CCN concentrations, aerosol mass loading, chemical composition and ambient visibility were obtained on a daily basis for correlation with the visibility measured in subsequent fogs or hazes associated with increasing ambient humidity. Additionally, the differences between the aerosol characteristics measured at the coastal and inland sites were investigated, and the utility of using the general wind field pattern to infer air mass aerosol characteristics was assessed.

The specific objectives of the program were to:

(1) Examine the feasibility of developing practical fog visibility predictive techniques using precursor aerosol information.

(2) Examine the feasibility of using precursor aerosol information to predict the visibility in hazes associated with periods of increasing relative humidity.

(3) Determine the changes in the aerosol chemical composition and CCN concentration between the coastal and inland site.

(4) Examine the relationship of the precursor aerosol chemical composition and CCN concentration to the orientation of the general wind field.

1

(5). Determine the chemical composition of fog water and unactivated in-fog nuclei during fog episodes at both sites. (This last objective could not be realized because the chemical concentrations in the fog water samples were below the sensitivity threshold of the analysis technique (particle induced x-ray emission). Additionally, due to the inadvertant sampling of fog droplets by the samplers for interstitial aerosol, analysis of in-fog unactivated aerosol was not possible.)

1.2 REPORT SUMMARY

Section 3 presents results of attempts to correlate precursor aerosol characteristics with visibility in subsequent fogs and hazes. A total of eight fogs and thirteen periods of increased humidity and reduced visibility occurred at the two sites during the field program which were suitable for analysis.

Section 3.1 provides a complete log of the fog events and episodes of significant increases in relative humidity evaluated in this report.

Section 3.2 discusses the use of precursor aerosol characteristics to predict the minimum visibility (averaged over 5 and 60 minute periods) in subsequent fogs. Ten precursor aerosol parameters were statistically evaluated for correlation to measured fog visibilities. The analysis indicated that, taken alone, none of these parameters was sufficiently well correlated to fog visibility to be useful as a visibility predictor. However, a strong correlation (r^2 = 0.95) was found to exist between the minimum fog visibility and a combination of two precursor parameters: the weight percent of elements Na and Cl in the aerosol, and the aerosol's total dry mass loading. A firm physical interpretation of the observed correlation cannot be given at this time; as only eight fog episodes were included in this analysis, additional studies will be needed to determine the significance of the relationship.

Section 3.3 evaluates the utility of using precursor aerosol information to predict the decrease in visibility associated with periods of increasing relative humidity and haze. The results revealed that while such techniques are, in principle, capable of providing a reliable visibility prediction, their utility in actual forecasting may often be limited. A basic assumption implied when using precursor aerosol information is that the precursor aerosol will be representative of the aerosol population at the time

2

of forecast verification. Unfortunately, significant changes with respect to aerosol concentration and composition occurring during the forecast period may often render the precursor aerosol nonrepresentative of the aerosol upon which haze ultimately develops. Accordingly, these techniques were found to be more applicable to the Nobska site, a remote coastal area of relatively constant aerosol, than for the Otis AFB site, an active inland area characterized by varying aerosol populations.

Section 4 presents a comparison of the aerosol data obtained from the coastal and inland sites. Analyses revealed that significant changes with respect to aerosol composition, hygroscopicity and concentration may occur as an air mass moves inland. Specifically, the coastal aerosol was found to have a greater percentage of elements Na and Cl, a lower percentage of elements S and Si, was more hygroscopic and generally had a lower particle concentration. The observed differences existing in the aerosol over the 20 km distance between the two sites, clearly demonstrate the need to account for such differences in any precursor aerosol predictive scheme.

The relationship of the mesoscale wind field to the ambient aerosol chemical composition and CCN concentration is presented in Section 5. For the coastal Nobska site, the MCIDAS streamline classifications properly reflected the aerosol characteristics for roughly two-thirds of the field program days. Periods for which the classifications were not indicative of aerosol characteristics appear to be associated with periods of flow transitions. During such transitional periods, aerosol changes lagged wind field changes by approximately one day. The use of trajectory, as opposed to streamline, analyses would likely be of greater utility during these transitional periods. For the inland Otis AFB site, natural and anthropogenic aerosol sources severely limited the utility of the wind field to infer ambient aerosol characteristics at that site.

Appendix A describes the field instrumentation, test site and general measurement schedule. Appendix B tabulates the precursor aerosol and in-fog data. Examples of various wind field patterns and their assigned classification are presented in Appendix C. Appendices D and E present plots of visibility, relative humidity, wind speed and wind direction as functions of time for the Otis AFB and Nobska sites respectively.

Specific conclusions based on the findings presented in this report are outlined in Section 2.

3

Section 2

CONCLUSIONS

2.1 DISCUSSION

A major finding of this program is the potential correlation between fog visibility and the chemical composition and mass loading of the precursor aerosol. In view of the limited data base however, and the known dependence of fog visibility on certain non-aerosol parameters, further study is required to confirm this finding.

Fog visibility is known to be dependent upon a variety of non-aerosol parameters. Fog supersaturation, for example, while certainly limited by the aerosol population, is also dependent upon the strength of the driving mechanisms, e.g., the magnitude of radiational cooling. Also, variations in supersaturation, and hence visibility, may occur near the surface due to variations in ground temperature and moisture content. The removal of fog droplets by natural vegetation also influences fog visibility. Hence, in addition to precursor aerosol information, certain non-aerosol parameters appear necessary for a general visibility prediction scheme. It may well be that the relationship between the precursor aerosol and fog visibility found in this data set is specific to the two measurement sites and that necessary non-aerosol features have been naturally assimilated into the data base. The acquisition of additional field data from the Nobska, Otis AFB and other sites is required to determine the significance and generality of this relationship.

Additionally the possibility exists that aerosol population changes, occurring after acquisition of the precursor aerosol data, masked potential aerosol-fog visibility relationships. While in-fog data were not available to confirm or dismiss this possibility, evidence of aerosol population changes were frequently seen in the data obtained during haze episodes. Therefore, in future studies to quantify this observation, quantitative aerosol samples should be drawn directly from within the fog for correlation to the attendant fog visibility and for assessment of the representativeness of the precursor aerosol to the aerosol present at the time of fog formation.

The utility of techniques using precursor aerosol characteristics to predict changes in visibility during periods of increasing humidity was found to be severely

4

limited by changes in the aerosol population with respect to concentration and composition which can occur during the forecast period. Thus, such techniques are generally applicable only to areas having relatively constant aerosol characteristics. An additional problem associated with the utility of these techniques is the requirement of an accurate forecast of relative humidity. The feasibility of making such a forecast, particularly in the range of 92-100% RH over which aerosol growth and hence, visibility is strongly dependent, must be considered.

2.2 CONCLUSIONS

The primary conclusions drawn from the program are:

(1) Limited field data suggests that a strong correlation ($r^2 = 0.95$) may exist between the minimum fog visibility and a combination of two precursor aerosol parameters: the weight percent of elements Na and Cl in the aerosol, and the aerosol's total dry mass loading. Further studies are required to examine the physical significance and generality of this relationship.

(2) Relatively simple devices, such as a humidified nephelometer, can provide a reasonable and practical prediction of the change in ambient visibility as a function of humidity for use in forecasting such changes under the assumption that the aerosol population remains unchanged.

(3) The utility of techniques using precursor aerosol characteristics to predict visibility during fogs or periods of increasing ambient relative humidity can be severely limited by changes in the aerosol population which can occur during the forecast period.

(4) Significant differences exist between the aerosol characteristics of the coastal and inland sites separated by only 20 km. Such differences would have to be accounted for in any predictive technique based on precursor aerosol measurements.

(5)   For the coastal Nobska site, the MCIDAS streamline flow patterns
        were found to properly reflect measured ambient aerosol
        characteristics on approximately two-thirds of the field program
        days. At the inland Otis AFB site, natural and anthropogenic aerosol
        sources severely limited the utility of the wind field to infer ambient
        aerosol characteristics.

Section 3
DISCUSSION OF FIELD STUDY RESULTS

3.1   LOG OF FOG EVENTS AND EPISODES OF SIGNIFICANTLY INCREASING RELATIVE HUMIDITY

During the course of the field program there were numerous fog events and periods of steadily increasing humidity. The sequence of these events can best be seen through the plots of visibility and relative humidity as functions of time presented in Appendices D and E. Also shown on these plots are the sample periods for the precursor and in-fog measurements. Table 1 presents a log of the specific episodes of fog and increasing relative humidity which were analyzed in this study.

The MRI nephelometer stationed at the Otis AFB site was inoperative prior to midday on 17 June, and, thus, light hazes which may have occurred prior to this time could not be evaluated. Additionally, light fog occurring on 14 June was not included in the analysis due to the lack of precursor aerosol samples and the prolonged period of drizzle and rain which preceded fog formation. Also, episodes of ground fog occurring at the Otis AFB site during the morning of 15 June were not included due to the shallow, patchy nature of these brief events.

During the field program, samples were obtained at both sites for determination of the chemical composition of fog water and the accompanying unactivated in-fog nuclei during fog episodes. However, because the chemical concentrations in the fog water samples were below the sensitivity threshold of the analysis technqiue (particle induced x-ray emission), and due to the inadvertant sampling of fog droplets by the samplers for interstitial aerosol, meaningful analysis of these samples was not possible.

3.2   PREDICTION OF FOG VISIBILITY BASED ON PRECURSOR AEROSOL CHARACTERISTICS

Table 2 presents the pre-fog and in-fog parameters corresponding to the eight fog episodes investigated. Pre-fog parameters include visibility, relative humidity, aerosol and CCN concentrations, aerosol chemical composition, mass loading and

7

Table 1

**LOG OF FOG EVENTS AND EPISODES OF SIGNIFICANT
INCREASES IN AMBIENT RELATIVE HUMIDITY**

DATE OF PRECURSOR AEROSOL MEASUREMENTS	SITE	TYPE OF EVENT AND MINIMUM MEASURED VISIBILITY
16 JUNE	OTIS NOBSKA	INCREASING RH FOLLOWED BY ADVECTION FOG; 270 m INCREASING RH FOLLOWED BY ADVECTION FOG; 70 m
17 JUNE	OTIS NOBSKA	INCREASING RH; 8080 m INCREASING RH FOLLOWED BY FOG; 90 m
18 JUNE	OTIS NOBSKA	INCREASING RH FOLLOWED BY ADVECTION FOG; 140 m ADVECTION FOG; 45 m
20 JUNE	OTIS NOBSKA	INCREASING RH; 6590 m INCREASING RH; 8410 m
21 JUNE	OTIS NOBSKA	INCREASING RH FOLLOWED BY RADIATION FOG; 90 m INCREASING RH; 970 m
22 JUNE	OTIS NOBSKA	INCREASING RH FOLLOWED BY ADVECTION FOG; 210 m INCREASING RH FOLLOWED BY ADVECTION FOG; 110 m
23 JUNE	OTIS	INCREASING RH; 13500 m
24 JUNE	OTIS	INCREASING RH; 12800 m

Table 2

SUMMARY OF PRE-FOG AND IN-FOG MEASUREMENTS

PRE-FOG MEASUREMENTS

SITE	DATE	AT TIME OF ASAS MEASUREMENT:					AEROSOL FILTER SAMPLES:				GENERAL WINDS		
		RH (%)	VISIBIL-ITY (m)	AITKEN (#/CC)	ASAS 0.15-3.0 (#/CC)	CCN @ 0.5% SS (#/CC)	Na+Cl (wt. %)	Si+S (wt. %)	DRY MASS LOADING (μg/m³)	HYGRO-SCOPICITY (M/M₀ @ 94%)	SPEED (m/s)	DIRECTION (DEG.)	TRAJECTORY (TYPE)*
OTIS	16-17 JUNE	82	38400	5100	2570	2080	26	56	60.4	3.4	7.1	228	3
NOBSKA	16-17 JUNE	87	2610	2100	3260	1340	77	13	68.8	8.6	9.9	247	3
NOBSKA	17-18 JUNE	86	25600	6050	533	743	32	50	34.2	5.0	6.5-2.0	255-037	4
OTIS	18-19 JUNE	75	20900	12000	-	1650	3	74	24.1	3.1	1.9	179	1
NOBSKA	18-19 JUNE	96	6380	4000	2320	760	11	66	14.7	3.9	1.6	230	1
OTIS	21-22 JUNE	70	28800	11000	482	1370	17	64	27.8	4.1	4.8	217	3
OTIS	22-23 JUNE	55	27100	5500	529	1340	4	77	34.5	3.4	2.7	180	2
NOBSKA	22-23 JUNE	68	17100	10800	708	1700	13	70	32.6	2.9	1.8	138	2

*TRAJECTORIES: 1 = MARINE; 2 = PRIMARILY MARINE; 3 = MIXED; 4 = PRIMARILY CONTINENTAL; 5 = CONTINENTAL

IN-FOG MEASUREMENTS

SITE	DATE	MIN. VISIBILITY		FSSP (60 minute AVERAGE)				
		5 MINUTE AVERAGE (m)	60 MINUTE AVERAGE (m)	0.5-2.5 (#/CC)	2.5-47 (#/CC)	LWC (g/m³)	MEAN DIAMETER (μm)	COMPUTED VISIBILITY (m)
OTIS	16-17 JUNE	271	302	254	16	1.14E-4	6.7	1690
NOBSKA	16-17 JUNE	72	77	518	296	1.49E-1	5.9	143
NOBSKA	17-18 JUNE	86	114					
OTIS	18-19 JUNE	138	160	190	70.8	2.16E-1	14.4	125
NOBSKA	18-19 JUNE	45	61	258	253	6.26E-1	10.1	52
OTIS	21-22 JUNE	93	139					
OTIS	22-23 JUNE	210	250	438	9.5	4.18E-3	5.2	2400
NOBSKA	22-23 JUNE	108	139	380	42.6	1.48E-2	5.6	1000

9

hygroscopicity, general wind speed and direction as well as an assessment of mesoscale wind trajectory.

Pre-fog aerosol measurements with AFGL's PMS probe (0.15-3.0 μm diameter) were generally made twice daily at each site. The measurement which most closely preceded fog formation was selected for inclusion in the pre-fog data base. Corresponding to the time of the selected PMS measurement, values of CCN concentration at 0.5% supersaturation, Aitken concentration, visibility and relative humidity were determined.

From aerosol filter samples collected over an ~8 hour period once daily at each site, the pre-fog aerosol chemical composition (Na to U), dry ambient mass loading and hygroscopicity were determined. Results of the chemical analyses indicate that the bulk of the aerosol consisted of four elements: Na, Cl, S, Si. In Table 2, the weight percents of Na + Cl and S + Si are used to provide a measure of the marine and continental character of the aerosol respectively.

For the overall pre-fog period, the general wind speed and direction were determined. Additionally, using the MCIDAS streamline analyses, the general air flow pattern was classified with respect to its marine or continental nature.

In-fog parameters, averaged over a 60 minute period, include minimum visibility and the droplet size distribution with associated calculations of liquid water content, mean particle diameter and visibility. Additionally, the minimum visibility averaged over a five minute period (as provided by AFGL's computer print out) is included. The exact time periods corresponding to the selected visibilities may be found in Appendix B. The visibility calculated from the measured in-fog droplet size distribution is included as a means of determining if the PMS measurement was made in dense fog. As can be seen by comparison of the computed visibilities to the measured minimum visibilities only three cases exist where PMS data were obtained in dense fog (Nobska 16-17 June, Otis and Nobska 18-19 June).

In addition to the measured precursor parameters presented in Table 2, other parameters were computed for correlation to fog visibility; these parameters, based on measurements of the pre-fog humidity, visibility and aerosol hygroscopicity, include:

10

o   calculated visibility at 5% RH

o   calculated visibility at 94% RH

o   calculated ambient mass loading at 94% RH.

Details on how these calculations were performed, which follow the techniques used to predict haze visibilities, are presented in Section 3.3.

Using the measured and computed precursor aerosol parameters, the statistical correlation between each parameter and the minimum fog visibility averaged over 5 and 60 minute periods was determined. Table 3 presents the correlation coefficients (r^2) resulting from this analysis. It is readily apparent from Table 3 that none of the precursor parameters, taken alone, was well correlated to fog visibility.

To investigate the possibility that a combination of precursor parameters might be correlated to fog visibility, a multiple linear regression analysis was performed for all possible pairs of the precursor parameters. The resultant correlation matrix is presented in Table 4. As can be seen, in most instances little improvement over the single parameter correlations was achieved. However, for the combination of the weight percent of elements Na and Cl in the precursor aerosol and the aerosol's total dry mass loading, correlations (r^2) of 0.95 and 0.94 to the subsequent measured minimum fog visibility averaged over a 5 and 60 minute period, respectively, were found. The equations relating these precursor parameters to fog visibility based on the combined Otis AFB and Nobska data are:

$$Y_1 = -3.09 - 4.68\ x_1 + 6.41\ x_2$$

and $$Y_2 = 24.4 - 5.20\ x_1 + 6.73\ x_2$$

where Y_1 = minimum fog visibility (m) averaged over a 5 minute period

Y_2 = minimum fog visibility (m) averaged overe a 60 minute period

x_1 = weight percent of elements Na and Cl in the precursor aerosol

x_2 = precursor aerosol dry mass loading ($\mu g/m^3$)

11

Table 3

COEFFICIENTS OF DETERMINATION (r^2) FOR PRECURSOR
AEROSOL PARAMETERS TO FOG VISIBILITY

PRECURSOR AEROSOL PARAMETER	CORRELATIONS TO MINIMUM FOG VISIBILITY ($r^2 \times 100$)	
	5 MINUTE AVERAGE	60 MINUTE AVERAGE
AITKEN PARTICLE CONCENTRATION	0	1
ASAS PARTICLE CONCENTRATION	0	2
CCN CONCENTRATION @ 0.5% SS	51	48
WT. % OF ELEMENTS Na + Cl	7	11
WT. % OF ELEMENTS S + Si	8	14
DRY MASS LOADING	14	9
COMPUTED MASS LOADING @ 94% RH	1	4
COMPUTED VISIBILITY @ 5% RH	16	18
COMPUTED VISIBILITY @ 94% RH	31	34
WIND FIELD CLASSIFICATION	0	1

Table 4. Correlation matrix of precursor aerosol parameter pairs to the 5 and 60 minute average minimum fog visibility, (r2 x 100).

5 MINUTE MINIMUM VISIBILITY

	ASAS PARTICLE CONCENTRATION	CCN CONCENTRATION @ 0.5% SS	WT. % OF ELEMENTS Na+Cl	WT. % OF ELEMENTS S+Si	DRY MASS LOADING	WIND FIELD CLASSIFICATION	COMPUTED MASS LOADING @ 94% RH	COMPUTED VISIBILITY @ 94% RH	COMPUTED VISIBILITY @ 5% RH
AITKEN PARTICLE CONCENTRATION	0	57	11	14	13	1	2	31	16
ASAS PARTICLE CONCENTRATION	–	54	11	15	26	1	2	34	18
CCN CONCENTRATION @ 0.5% SS	–	–	55	55	51	53	53	73	72
WT. % OF ELEMENTS Na+Cl	–	–	–	19	(95)	14	31	32	18
WT. % OF ELEMENTS S+Si	–	–	–	–	91	16	54	32	20
DRY MASS LOADING	–	–	–	–	–	16	92	50	33
WIND FIELD CLASSIFICATION	–	–	–	–	–	–	13	32	16
COMPUTED MASS LOADING @ 94% RH	–	–	–	–	–	–	–	35	16
COMPUTED VISIBILITY @ 94% RH	–	–	–	–	–	–	–	–	61
COMPUTED VISIBILITY @ 5% RH	–	–	–	–	–	–	–	–	–

60 MINUTE MINIMUM VISIBILITY

	ASAS PARTICLE CONCENTRATION	CCN CONCENTRATION @ 0.5% SS	WT. % OF ELEMENTS Na+Cl	WT. % OF ELEMENTS S+Si	DRY MASS LOADING	WIND FIELD CLASSIFICATION	COMPUTED MASS LOADING @ 94% RH	COMPUTED VISIBILITY @ 94% RH	COMPUTED VISIBILITY @ 5% RH
AITKEN PARTICLE CONCENTRATION	2	50	13	17	16	2	4	35	20
ASAS PARTICLE CONCENTRATION	–	57	14	17	25	3	4	36	20
CCN CONCENTRATION @ 0.5% SS	–	–	56	56	48	50	54	75	71
WT. % OF ELEMENTS Na+Cl	–	–	–	26	(94)	23	36	36	23
WT. % OF ELEMENTS S+Si	–	–	–	–	91	26	36	37	26
DRY MASS LOADING	–	–	–	–	–	9	93	47	29
WIND FIELD CLASSIFICATION	–	–	–	–	–	–	9	35	19
COMPUTED MASS LOADING @ 94% RH	–	–	–	–	–	–	–	35	18
COMPUTED VISIBILITY @ 94% RH	–	–	–	–	–	–	–	–	62
COMPUTED VISIBILITY @ 5% RH	–	–	–	–	–	–	–	–	–

13

Using the above expressions, Figure 1 was prepared showing the relationship of the predictive to measured visibilities.

Due to the limited number of fogs comprising this analysis, the apparent correlation must be viewed cautiously. While it is very likely that an aerosol's mass loading and chemical composition are parameters of significance relative to fog visibility, a well defined physical interpretation of the above relationships cannot, at present, be given. The possibility that changes in the aerosol population, occurring after acquisition of the precursor aerosol sample, precluded more direct, one parameter, correlations cannot be dismissed. Thus, to examine this relationship in future studies, quantitative aerosol samples should be drawn directly from fog for correlation to the attendant fog visibility and for comparison to the precursor aerosol. Additionally, the generality of these relationships with respect to their application to sites other than Otis AFB and Nobska locations needs to examined.

3.3   THE UTILITY OF PRECURSOR AEROSOL INFORMATION IN HAZE VISIBILITY PREDICTION

As a consequence of the inherent hygroscopicity of ambient aerosol, significant reductions in visibility can occur during periods of increasing relative humidity. To examine the feasibility of predicting this humidity dependent reduction in visibility, two techniques were employed. The two methods are discussed below, and visibility predictions as functions of humidity are compared with observations in Figure 2.

During precursor aerosol sampling periods, a direct measure of the change in visibility with increasing humidity was obtained by humidification of the aerosol inlet to the MRI nephelometer stationed at the Otis AFB site. Humidification took place over an approximate 20 minute period during which the humidity was increased from the ambient level to $\sim$90% RH; the maximum humidity attainable with the apparatus. Visibility vs. relative humidity data from this method are shown as the dotted lines in Figure 2.
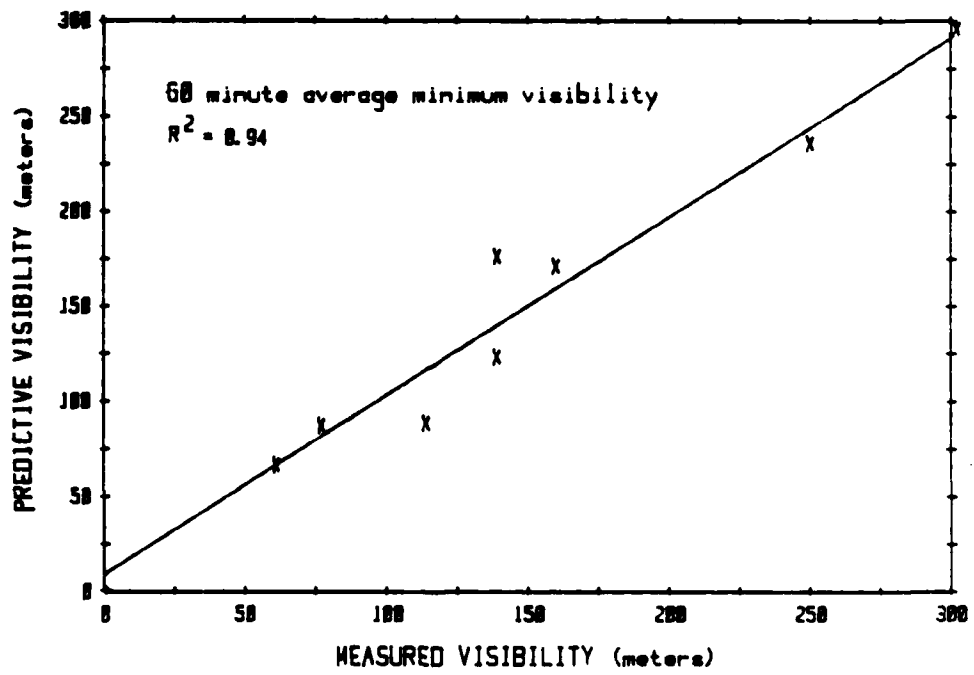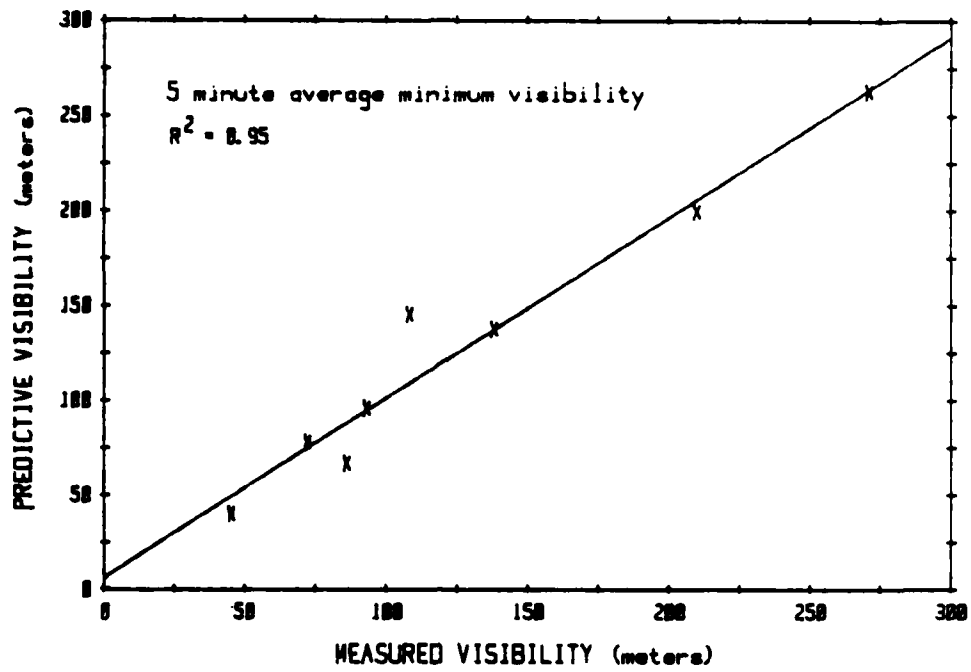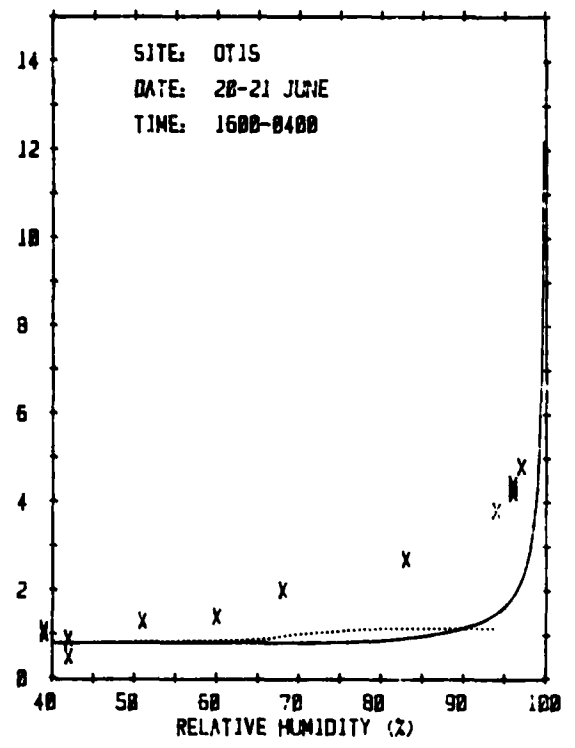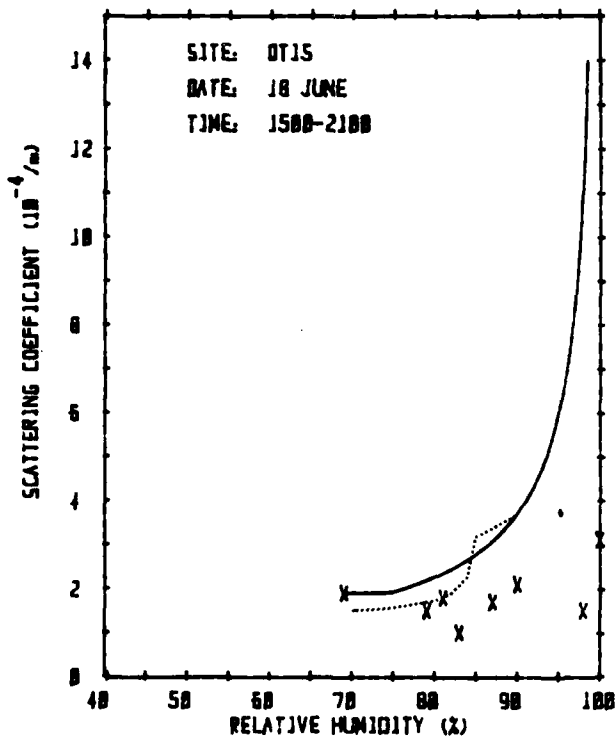
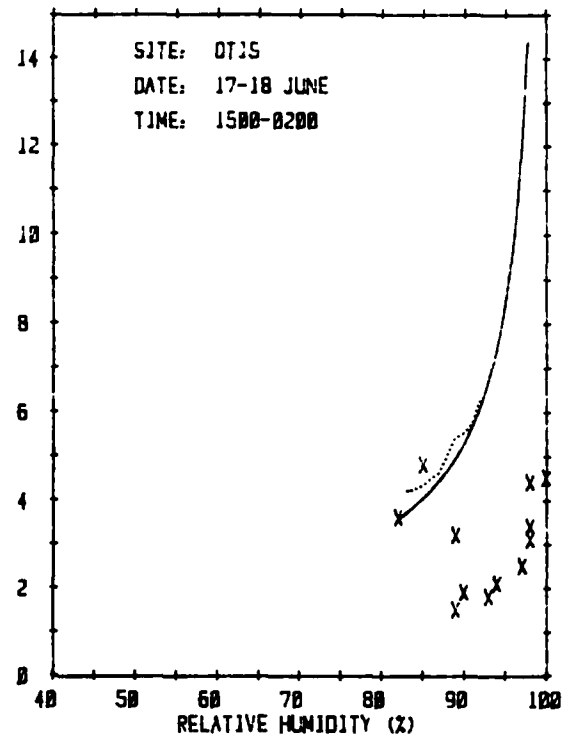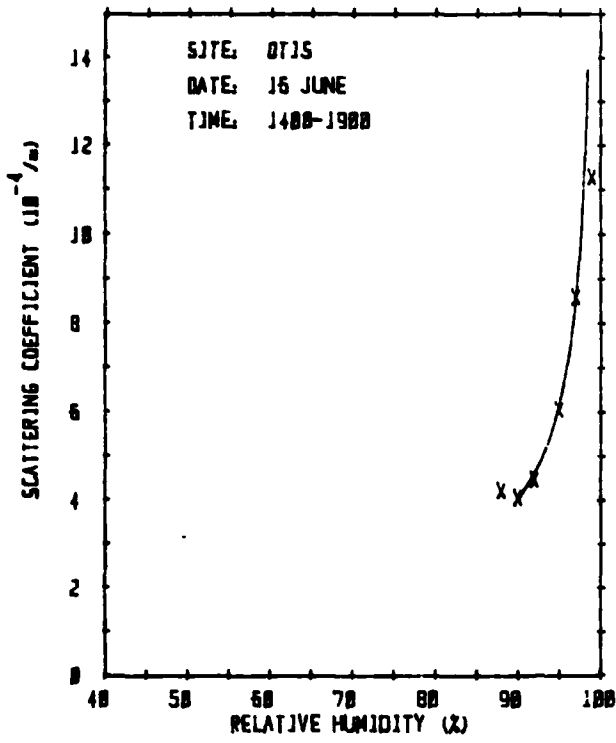Figure 1.   Predictive vs. Measured Visibility

15

Figure 2.   Scattering coefficient as a function of increasing relative humidity.
X = Observed   .... = MRI Prediction   —— = M/Mo Prediction

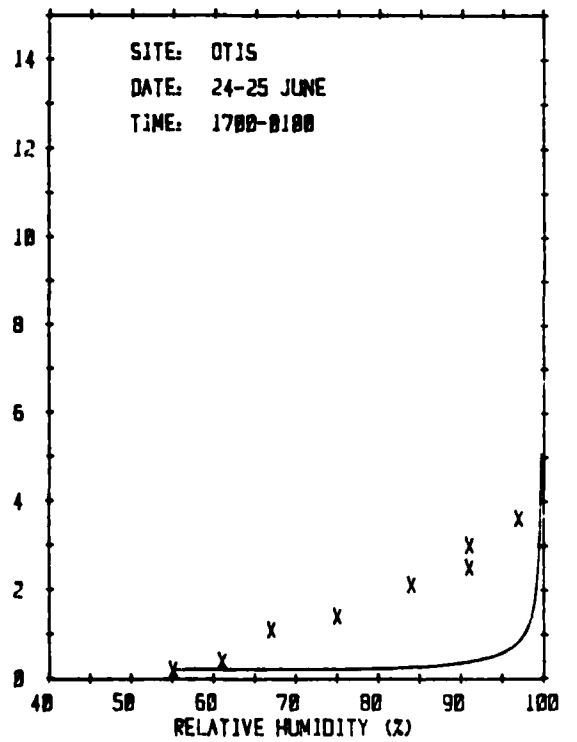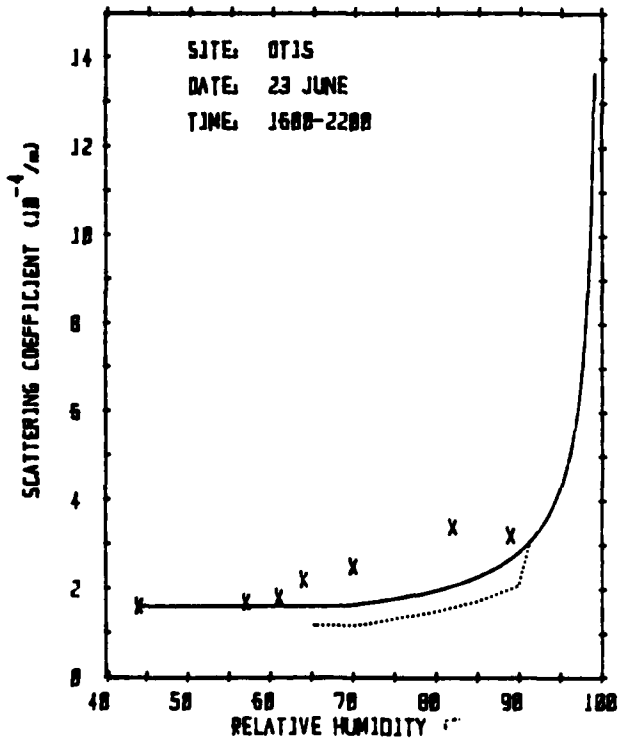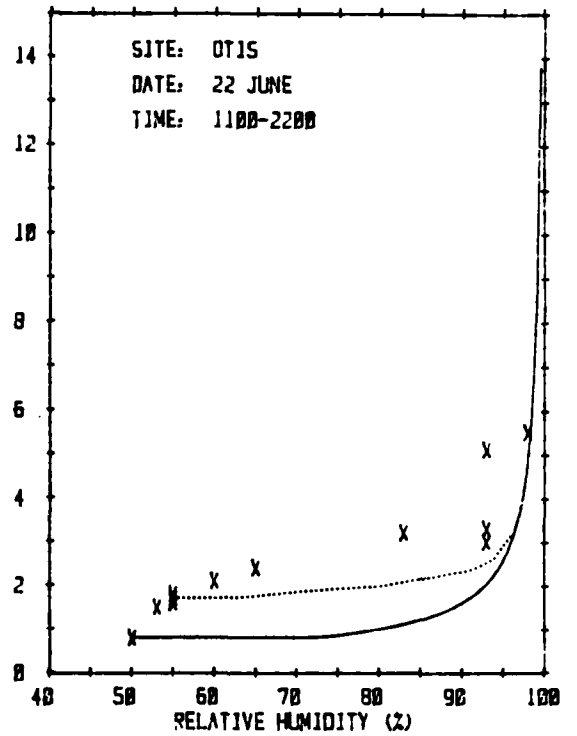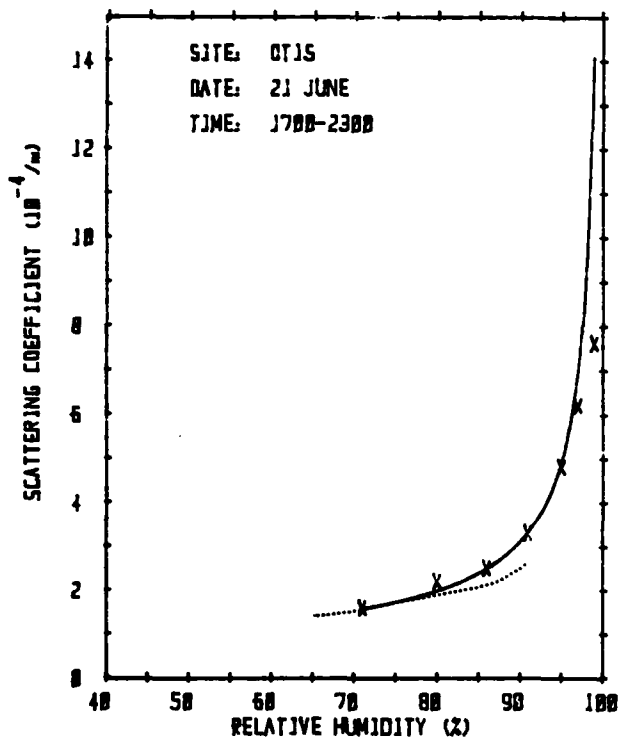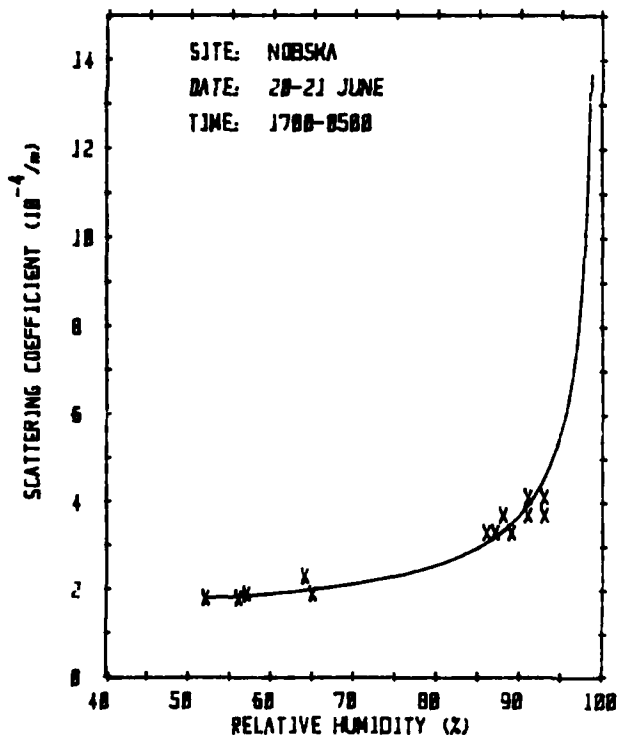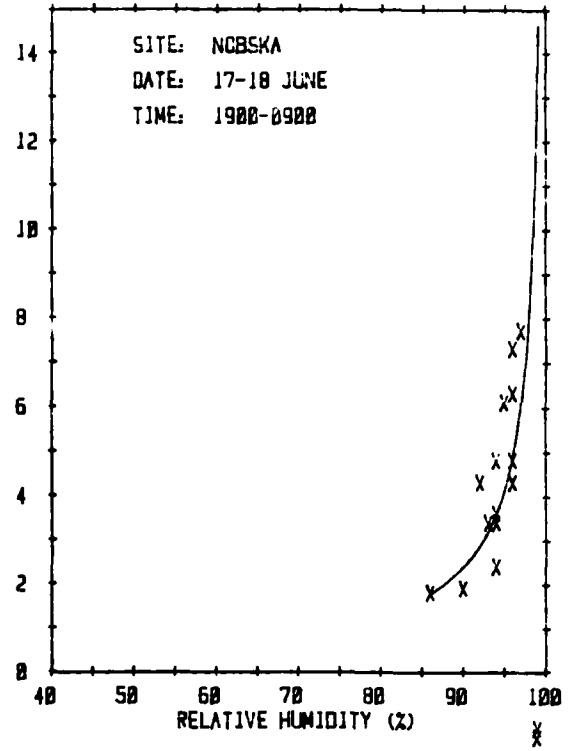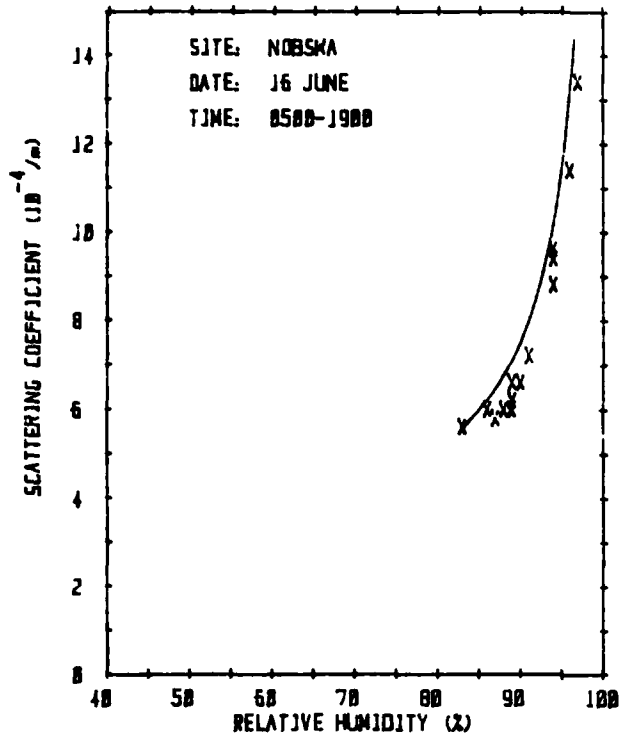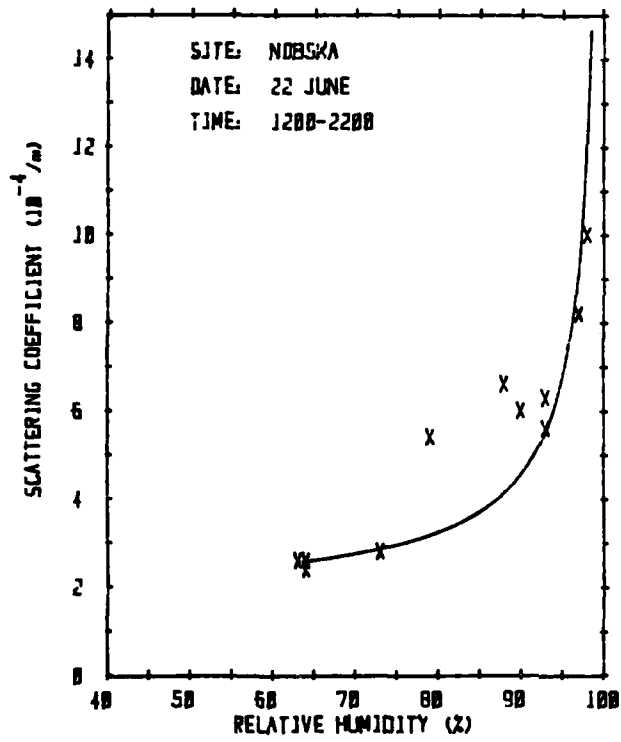Figure 2. Continued

17

Figure 2. Continued

18

Figure 2.   Continued

19
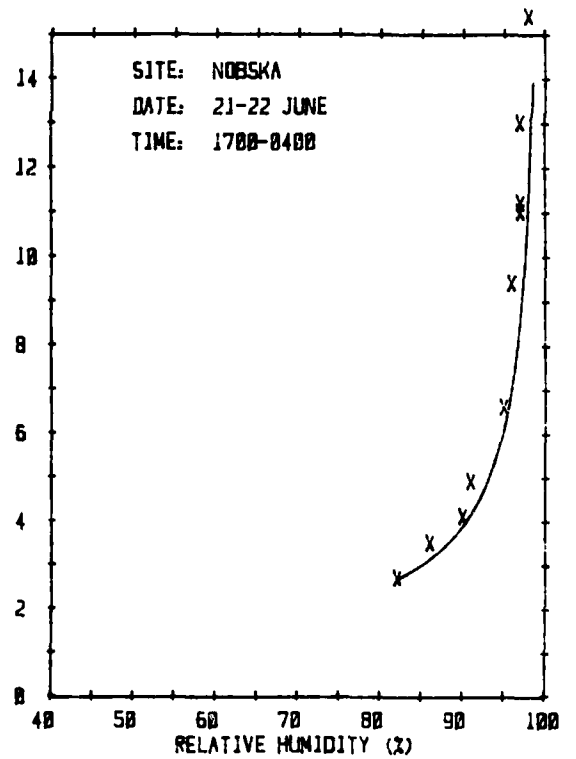
An additional procedure for predicting visibility as a function of humidity was based on the hygroscopicity of the aerosol and a measure of visibility and humidity during the precursor sampling period. Aerosol hygroscopicity was determined by weighing aerosol filter samples as a function of increasing relative humidity from 5 to 98%. These data are presented in Appendix B. Analysis of these data revealed that the ratio of the aerosol sample mass at a given humidity (M) to the dry sample mass (M_0) could be expressed as:

$$M/M_0 = a + b/(1-RH) \qquad (1)$$

where a and b are constants for each aerosol sample determined by a least squares fitting routine and RH is expressed in decimal form. This expression fit the hygroscopicity data for the samples with an average r^2 value of 0.975. Through the use of two aditional relationships, the aerosol hygroscopicity (M/M_0) was used to compute visibility as a function of humidity as outlined below.

An aerosol's scattering coefficient is directly related to its cross sectional area and hence to the square of its radius. It therefore follows (Charlson et al, 1978)[*] that the ratio of the scattering coefficient at a given humidity (β) to the value at low humidity (β_0) is equal to the square of the corresponding radius ratio: $\beta/\beta_0 = (r/r_0)^2$. Furthermore, since a particle's mass is proportional to the cube of its radius, and assuming particle density to be constant, then $(r/r_0)^3 = M/M_0$. Combining these relations and expressing the scattering coefficient in terms of visibility yields an expression relating a change in visibility to a change in hygroscopicity:

$$V = V_0 \, (M/M_0)^{3/2} \qquad (2)$$

Thus, given initial values of visibility and relative humidity obtained during the precursor aerosol sampling period, and having determined the values of a and b of equation (1) from the aerosol hygroscopicity analysis, equations (1) and (2) were used to compute ambient visibilities as a continuous function of increasing relative humidity up to 98% RH.

---

[*]Charlson R.J., Covert, D.S., Larson, T.V. and Waggoner, A.P. (1978) Chemical Properties of Tropospheric Sulfur Aerosol. Atmospheric Environment, Vol. 12, pp 39-53.

Figure 2 presents the measured ambient visibilities along with the predicted visibilities based on both methods discussed above for each of the 13 periods of increasing humidity observed on the field program. As can be seen, the accuracy of the predictions differs from case to case. For most cases where the prediction does not match observation, the cause can be linked to significant changes in concentration and/or composition of the aerosol population. Both of these predictive schemes assume that visibility changes will be solely dependent upon relative humidity, and both predicted similar changes in visibility (based on reactions of the same precursor aerosol to humidity increases). However, changes in visibility may also occur due to gross changes in aerosol population associated with anthropogenic activity and natural phenomena such as wind shifts and frontal passages. If such events occur after the precursor measurements have been made, the prediction will likely be poor since the precursor aerosol is no longer representative of the aerosol population at the time of forecast verification.

For a constant aerosol population, visibility will decrease with increasing humidity. If this relationship is not reflected in field observations, as occurs in several plots of Figure 2, it is evidence of a changing aerosol population. It is apparent from the figures that the visibility predictions were generally more accurate for the Nobska site than for the Otis AFB location. This is likely a reflection of the comparitively constant aerosol population of the remote coastal Nobska site relative to the more variable aerosol of the inland Otis AFB location, a semi-active military base. Table 5 summarizes the prediction results and comments on the representativeness of the precursor aerosol for each data set.

Both predictive techniques employed assume that constant aerosol characteristics are maintained through the forecast period. Reflecting this assumption, the data suggests that such techniques are more applicable to locations having relatively stable aerosol characteristics. In other locations, the utility of these techniques may be severely limited by changes in the aerosol characteristics during the forecast period.

21

Table 5

SUMMARY OF VISIBILITY PREDICTIONS FOR PERIODS OF SIGNIFICANTLY INCREASING RELATIVE HUMIDITY

SITE	DATE	TIME OF HUMIDITY INCREASE	DOES PREDICTION MATCH OBSERVATION?	DO OBSERVATIONS SUGGEST A CONSTANT AEROSOL POPULATION?	COMMENTS RELATIVE TO AEROSOL POPULATION CHANGES
OTIS	16 JUNE	1400 - 1900	YES	YES	
OTIS	17-18 JUNE	1500 - 0200	NO	NO	FRONTAL PASSAGE. PLOTTED DATA INDICATES THAT CHANGES IN VISIBILITY WERE NOT SOLELY A FUNCTION OF CHANGES IN RH.
OTIS	18 JUNE	1500 - 2100	NO	NO	PLOTTED DATA REVEALS THAT VISIBILITY CHANGES WERE NOT SOLELY A FUNCTION OF CHANGES IN RH.
OTIS	20-21 JUNE	1600 - 0400	NO	NO	GENERAL WIND SHIFT FROM W TO SW AFTER PRECURSOR AEROSOL SAMPLE PERIOD MAY HAVE ALTERED AEROSOL POPULATION.
OTIS	21 JUNE	1700 - 2300	YES	YES	
OTIS	22 JUNE	1100 - 2200	NO	NO	PLOTTED DATA REVEALS THAT VISIBILITY CHANGES WERE NOT SOLELY A FUNCTION OF CHANGES IN RH.
OTIS	23 JUNE	1600 - 2200	NO	NO	PLOTTED DATA REVEALS THAT VISIBILITY CHANGES WERE NOT SOLELY A FUNCTION OF CHANGES IN RH.
OTIS	24-25 JUNE	1700 - 0100	NO	NO	INCREASING CCN CONCENTRATION SUGGESTS AEROSOL POPULATION WAS NOT CONSTANT.
NOBSKA	16 JUNE	0500 - 1900	YES	YES	
NOBSKA	17-18 JUNE	1900 - 0900	YES	NO	REASONABLE PREDICTION DISPITE FRONTAL PASSAGE.
NOBSKA	20-21 JUNE	1700 - 0500	YES	YES	
NOBSKA	21-22 JUNE	1700 - 0400	YES	YES	
NOBSKA	22 JUNE	1200 - 2200	YES/NO	NO	VARIABLE WINDS. PLOTTED DATA REVEALS THAT VISIBILITY CHANGES WERE NOT SOLELY A FUNCTION OF CHANGES IN RH.

Section 4

AIR MASS AEROSOL MODIFICATION OCCURRING BETWEEN
THE COASTAL AND INLAND SITES

Using data obtained at the coastal (Nobska) and inland (Otis AFB) sites, the changes in aerosol population as air masses moved inland from the coast were investigated. Figure 3 presents scatter plots of various aerosol characteristics (chemical composition, mass loading, hygroscopicity and CCN concentration) for the two sites. Periods during which the air flow was not onshore at Nobska have been eliminated.

As can be seen by the plots, significant differences existed between the coastal and inland aerosol. The coastal aerosol generally had a greater weight percent of elements Na and Cl, a lower percentage of elements S and Si, was more hygroscopic and had a lower particle concentration. CCN concentration appeared to be slightly greater for the inland site. No systematic difference in the total aerosol dry mass loadings of the two sites was observed.

As a specific example of the changes which occurred in the aerosol characteristics as an air mass traveled from the coastal to inland sites, Table 6 presents the precursor aerosol data obtained on 16 June 1982. This date was selected for the steady southwest winds which prevailed thereby placing Nobska in an onshore flow directly upwind of Otis AFB. As can be seen, as the air mass moved inland, both the Aitken and CCN concentrations increased by approximately a factor of two, the aerosol composition changed from predominantly Na + Cl to S + Si and aerosol hygroscopicity dropped 60% from 8.6 down to 3.4. Dry mass loading for the two sites was roughly equivalent.

The two measurement sites are separated by a distance of $\sim$20km. Due to the differences in the aerosol observed at the two sites, care must be used in defining the limits of the forecast area. Otherwise, a precursor aerosol measurement may be applied to areas outside its region of representativeness.
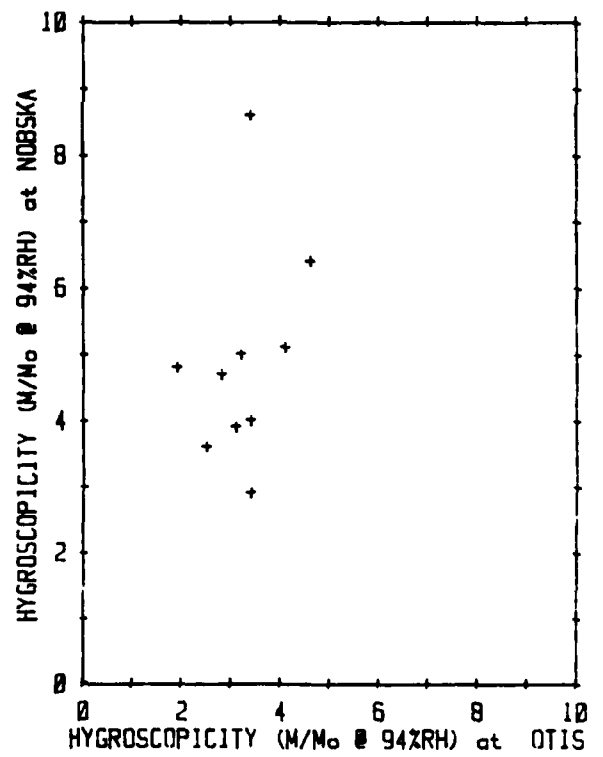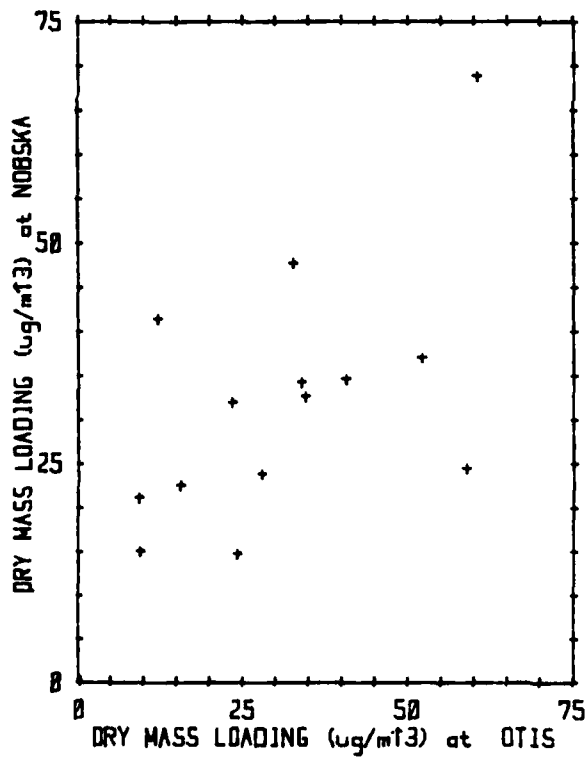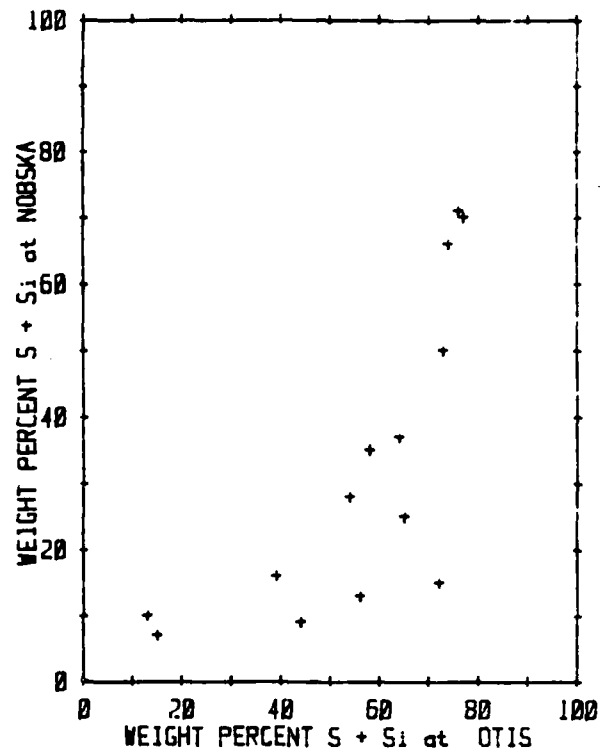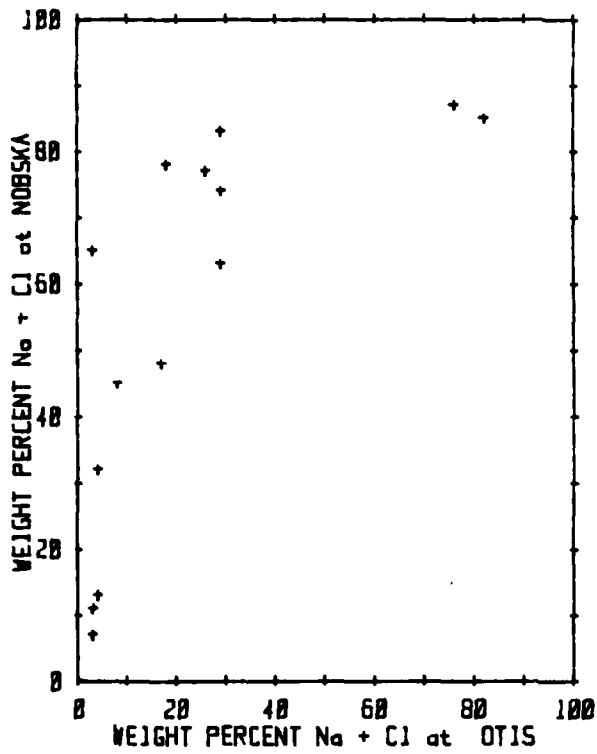
Figure 3.   Correlation plots between various precursor aerosol parameters
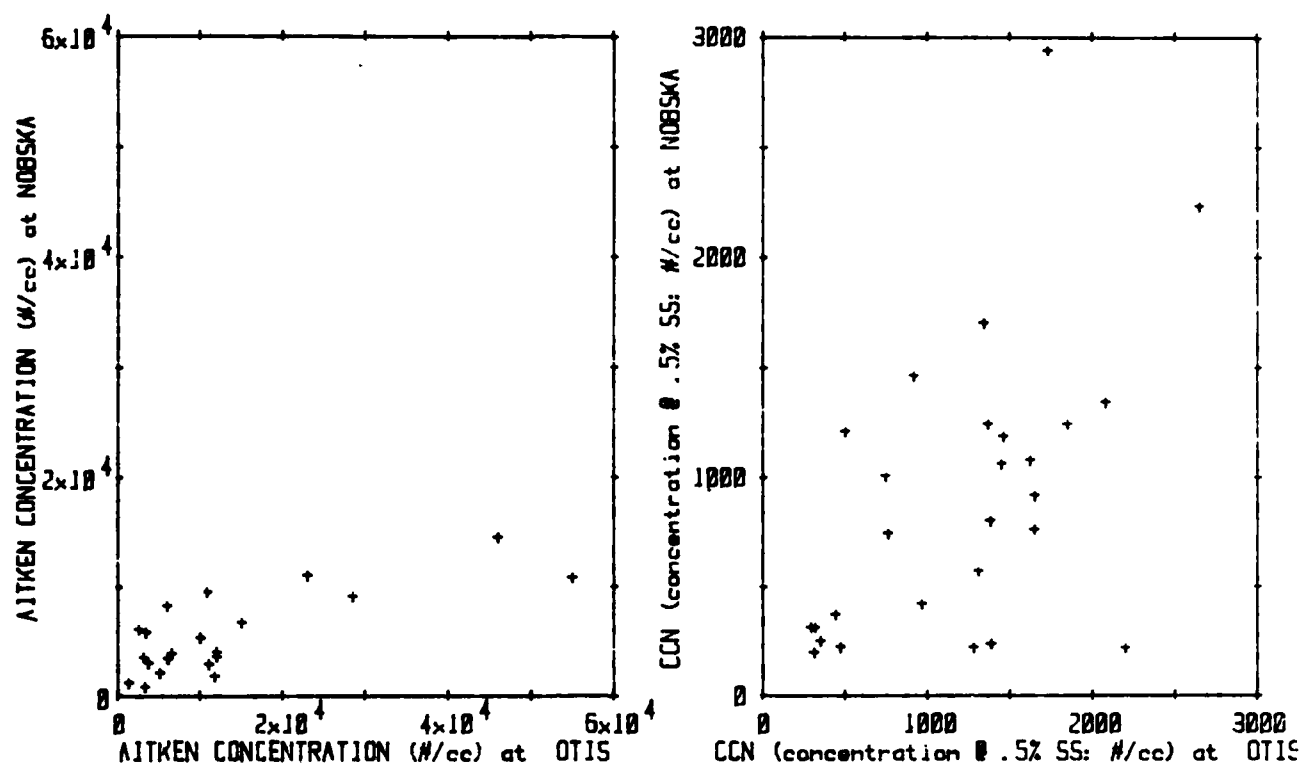   for the Nobska and Otis AFB site.

24

Figure 3.   Continued.

Table 6

COMPARISON OF PRECURSOR AEROSOL CHARACTERISTICS
FOR THE NOBSKA AND OTIS AFB SITES ON 16 JUNE

| PRECURSOR PARAMETER	NOBSKA	OTIS
AITKEN CONCENTRATION (#/cc)	2100	5100
CCN CONCENTRATION @ 0.5% SS (#/cc)	1340	2080
WT. % OF ELEMENTS Na + Cl	77	26
WT. % OF ELEMENTS S + Si	13	56
HYGROSCOPICITY (M/Mo @ 94% RH)	8.6	3.4
DRY MASS LOADING (μ g/m^3)	68.8	60.4

Section 5

THE UTILITY OF THE GENERAL WIND FIELD TO
INFER AMBIENT AEROSOL CHARACTERITICS

For the period of the field program, the utility of using the general wind field to infer ambient aerosol chemical composition and CCN concentrations was investigated. In general, high NaCl aerosol content and low CCN concentration are characteristic of a marine environment; conversely, low NaCl and high CCN values characterize a continental environment. Classification of the wind field was based on mesoscale streamline analyses of surface winds over the Northeast United States provided by AFGL's MCIDAS system. These analyses were provided three times daily at 1200, 1700 and 2200 EDT. For each streamline pattern, the airflow over the test area (i.e., Cape Cod) was classified as either Marine, Primarily Marine, Mixed, Primarily Continental or Continental. Appendix C presents examples of each of these classifications. The relationship of the wind field to aerosol composition and CCN concentration for the Otis and Nobska sites is presented in Figures 4 a-d. The daily wind field classifications noted in the figures are composites based on the three daily analyses.

As can be seen from the figures, a steady maritime flow prevailed from 9-14 June. On 15 June, the wind field shifted from a northeasterly Primarily Marine flow to a southwesterly Primarily Marine flow. During this transition, the flow became Continental for several hours, as can be seen in Appendices D and E. However, this Continental flow period occurred between output times of the provided MCIDAS analyses and was thus not observed in the streamline patterns. For the remaining period, 16-25 June, the wind field classification changed frequently, in contrast to the steady period of 9-14 June.

For the period 9-17 June, Nobska's CCN and NaCl values properly reflect the corresponding maritime flow as well as the Continental flow associated with the 15 June transition period discussed above. However, for the period 18-25 June, the Nobska NaCl values are not indicative of the accompanying flow classifications. For this latter period, changes in the NaCl values appear to lag changes in the wind field by approximately one day. As a consequence of this lag, higher NaCl values were actually observed during periods classified as Continental than during periods of maritime flow. A similar lag can be seen in Nobska's CCN concentrations for the period 20-25 June.
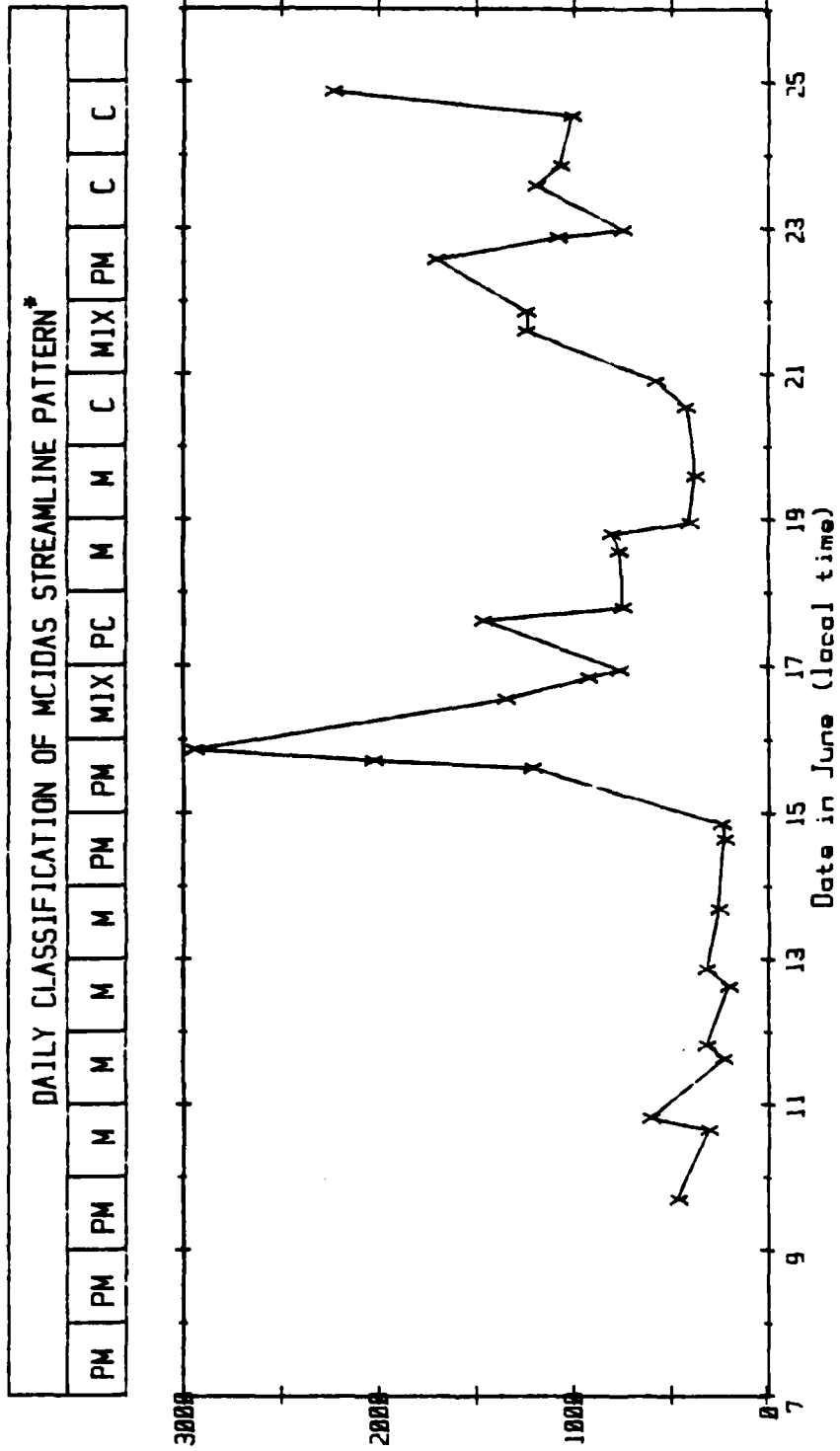
27
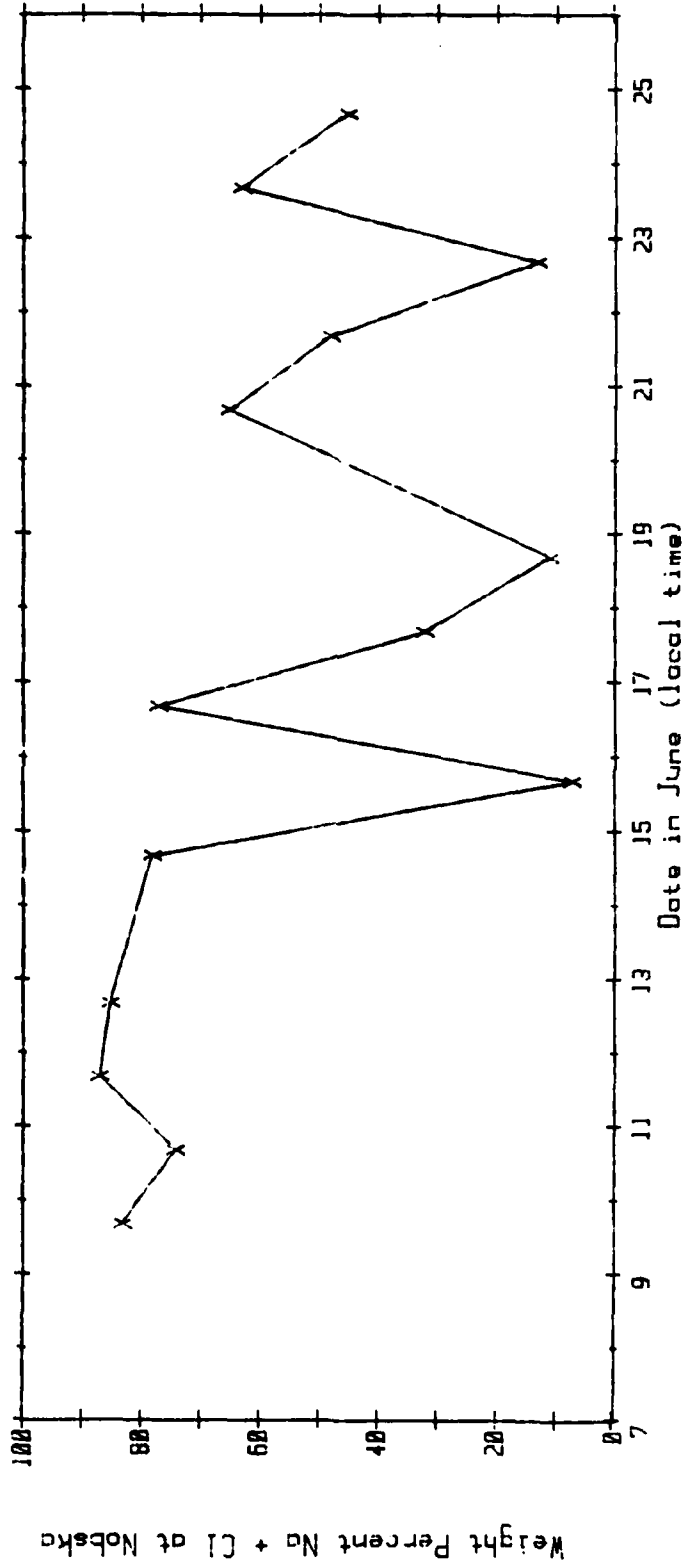
Figure 4a.   Relationship of MCIDAS streamline pattern to aerosol weight percent
of the elements Na + Cl at Nobska.

* M = marine,   PM = primarily marine,   MIX = mixed marine/continental,
PC = primarily continental,   C = continental

28

DAILY CLASSIFICATION OF MCIDAS STREAMLINE PATTERN*

PM	PM	PM	M	M	M	PM	PM	MIX	PC	M	M	C	MIX	PM	C	C

CCN (concentration at .5% SS; #/cc) at Nobska

Date in June (local time)

* M = marine, PM = primarily marine, MIX = mixed marine/continental,
PC = primarily continental, C = continental

Figure 4b.   Relationship of MCIDAS streamline pattern to CCN concentration at
.5% supersaturation at Nobska.

29

DAILY CLASSIFICATION OF MCIDAS STREAMLINE PATTERN*

| PM | PM | PM | M | M | M | M | PM | PM | MIX | PC | M | M | M | C | MIX | PM | C | C |

Weight Percent Na + Cl at Otis

Date in June (local time)

* M = marine, PM = primarily marine, MIX = mixed marine/continental,
PC = primarily continental, C = continental

Figure 4c.   Relationship of MCIDAS streamline pattern to weight percent of the
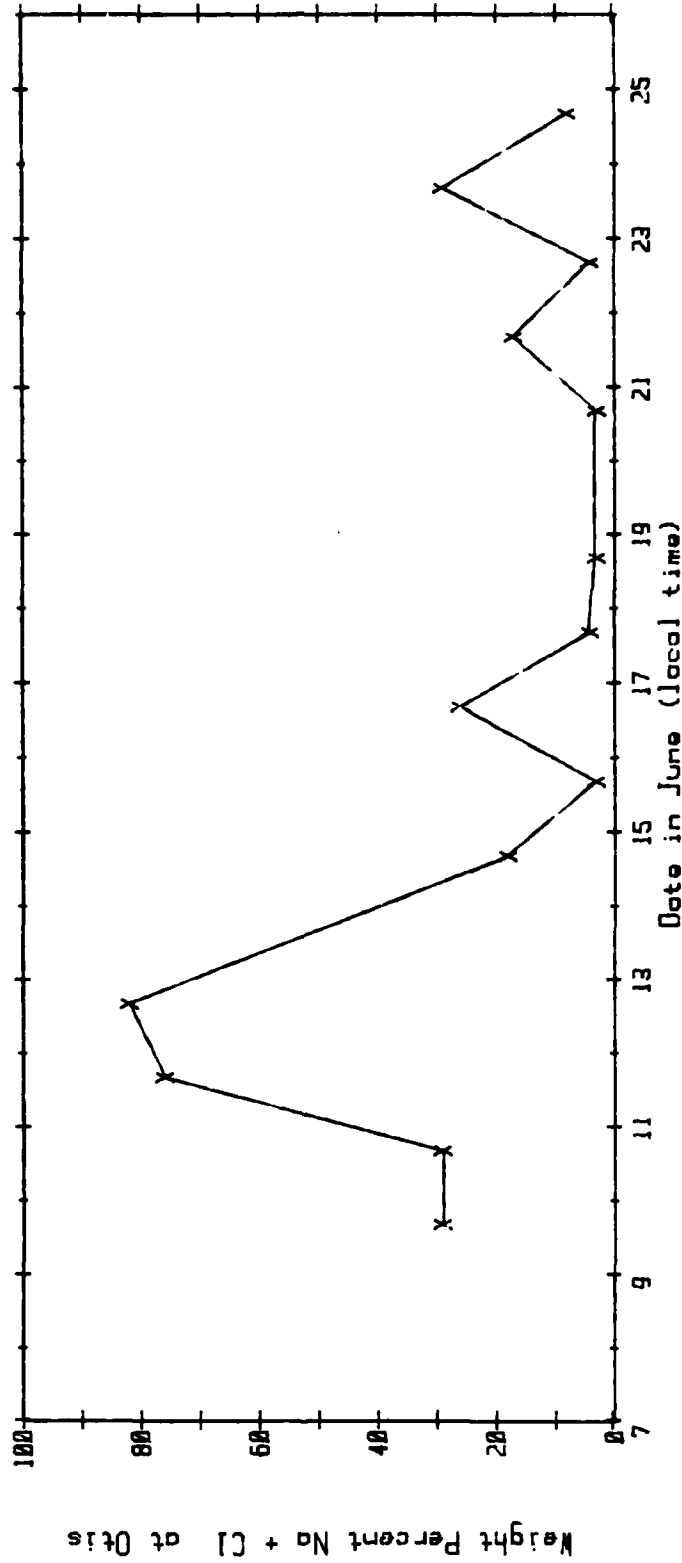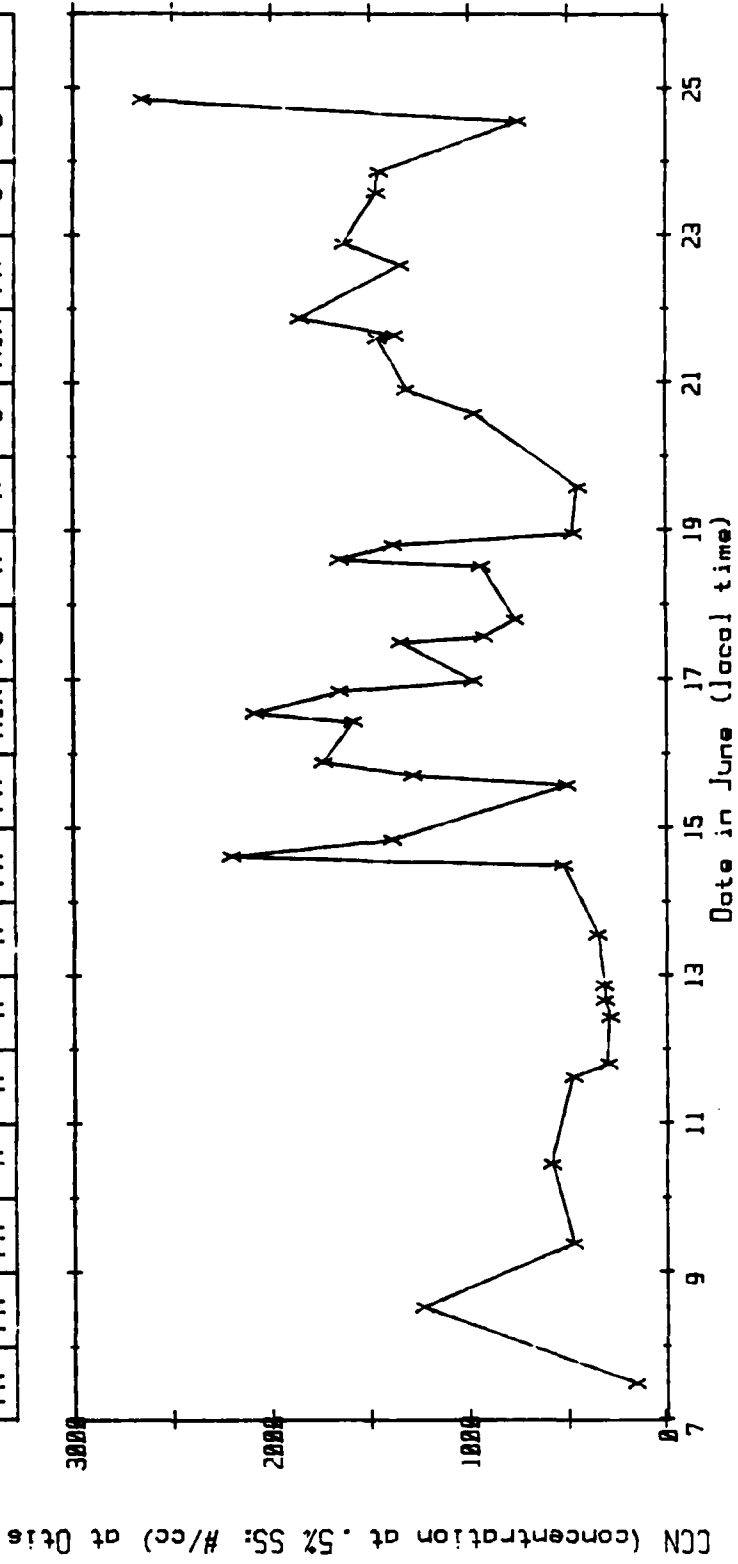elements Na + Cl at Otis.

30

DAILY CLASSIFICATION OF MCIDAS STREAMLINE PATTERN*

PM	PM	PM	M	M	M	M	PM	PM	PM	MIX	PC	M	M	M	C	MIX	PM	C	C

* M = marine, PM = primarily marine, MIX = mixed marine/continental,
PC = primarily continental, C = continental

Figure 4d. Relationship of MCIDAS streamline pattern to CCN concentration
at .5% supersaturation at Otis.

31

The observed lag in aerosol characteristics relative to wind field changes at the Nobska site is seen as a consequence of the time which is required to "flush out" an aerosol population associated with a previous flow pattern before the aerosol becomes representative of a new flow regime. For example, if after several days of Continental flow at Nobska, the flow became Marine, the aerosol would not immediately become marine in character. Rather, because continental aerosol had been carried out to sea during the period of Continental flow, the Marine flow would, for some period, also contain continental aerosol. Therefore, flow trajectories, as opposed to streamlines, may be of greater utility in inferring aerosol characteristics, particularly during periods of flow transition.

Thus, for the coastal Nobska site, the MCIDAS streamline classifications properly reflected the aerosol NaCl and CCN values for roughly two-thirds of the field program days. Periods for which the classifications were not indicative of aerosol characteristics appear to be associated with periods of flow transitions. During these transitional periods, aerosol changes lagged wind field changes by approximately one day. The use of trajectory, as opposed to streamline, analyses would likely be of greater utility during these transitional periods.

For the Otis AFB site, with the exception of 11 and 12 June, the NaCl values were always low, characteristic of a continental aerosol, and did not reflect changes in the MCIDAS wind field classifications. The low Otis AFB CCN values for the period 7-14 June reasonably reflect the accompanying maritime flow, however, after that period, the CCN values appear poorly correlated to the wind field. It is apparent that natural aerosol sources and anthropogenic activity at Otis AFB and the surrounding communities had a significant impact on the ambient aerosol characteristics, thereby severely limiting the utility of the mesoscale wind field to infer aerosol characteristics at this inland site.

Appendix A
TEST SITE, INSTRUMENTATION AND GENERAL MEASUREMENT SCHEDULE

The field study was conducted during the period 6 to 27 June 1982. Set-up of instrumentation and limited data acquistiion was initiated on 6 June; a full measurements schedule was begun by 9 June and continued thereafter on a daily basis. A map of the overall test area is presented in Figure A-1.

The measurement, instrumentation and observation schedules carried out during the program are summarized in tables A-1 and A-2. Measurements with AFGL instrumentation were recorded by the Data Acquisition System of the Wx Test Facility. In addition, the visibility and winds (measured by AFGL equipment) at both the Otis AFB and Nobska sites were continuously recorded on strip charts. Other observations were obtained as indicated in Table A-2.

Three basic measurement periods were planned for each day's operation: two pre-fog sequences, during the times ~ 1300 - 1530 EDT and 1800 2000 EDT; and one after mature fog developed. The weather facilities of the National Guard at Otis AFB was used to help prepare the specific measurement schedule for each day. If mature fog did not occur or appear imminent by ~ 0100, a third set of "pre-fog" measurements were obtained. At that time, a determination of the likelihood of fog occurrence was made followed by a decision relative to termination of the night's activities.
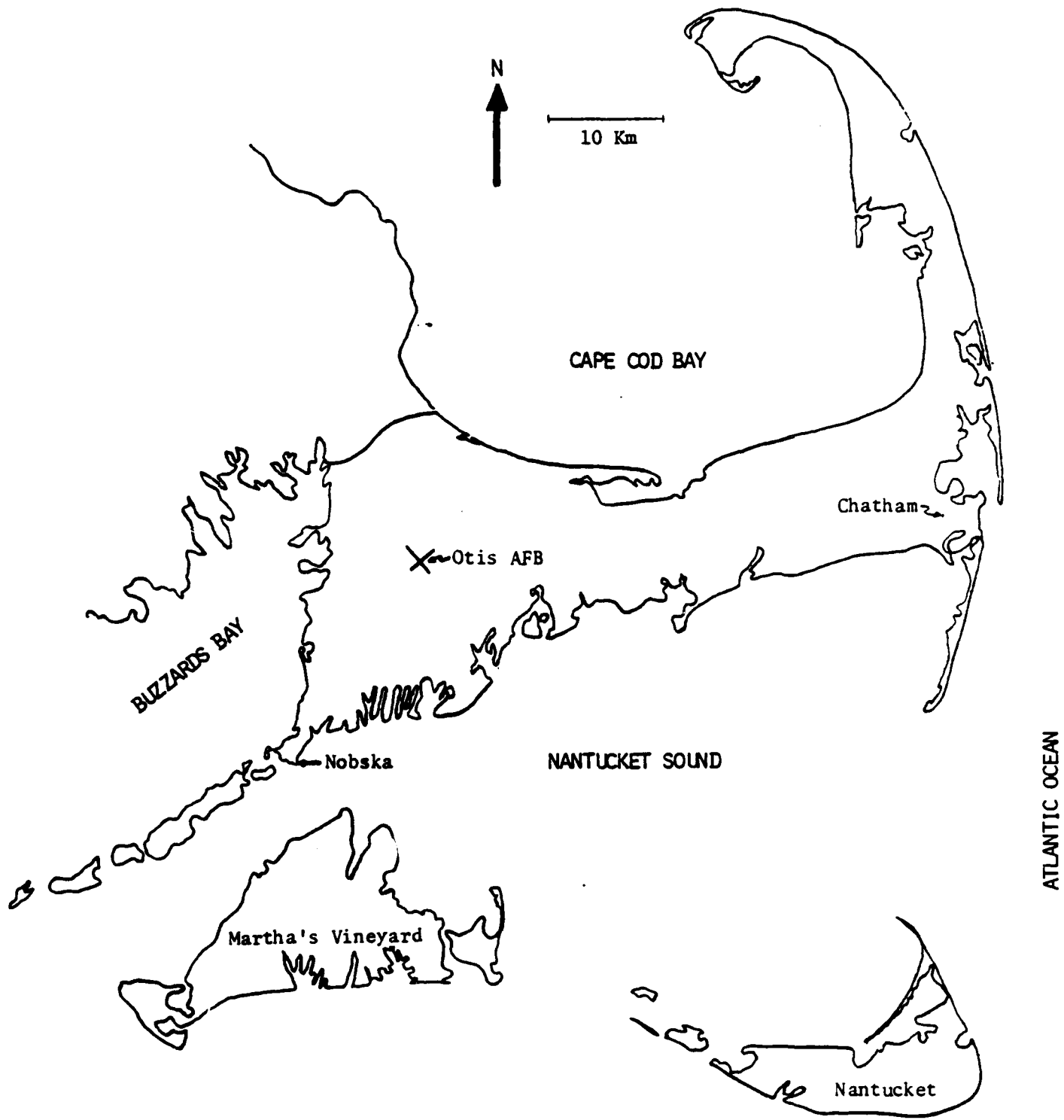
Figure A-1.   Otis AFB and Nobska test sites and surrounding area.

Table A-1

MEASUREMENTS AND INSTRUMENTATION

Parameter	Instrument
Visibility vs. RH (prediction)	Calspan-fab Humidification System for MRI Integrating Nephelometer
Visibility (clear air & haze)	MRI Integrating Nephelometers Model 2050 (one is AFGL instr)
Visibility (fog & dense haze)	EG&G Forward Scatter Meters Model 107 (AFGL instrumentation)
Total Particle Conc	Gardner Small Particle Detectors
CCN/Haze Nuc. Conc	Calspan-fab Thermal Gradient Diffusion Chambers
Individual Particle Chem	Casella Cascade Impactor and SEM Analysis
Quantitative Aerosol Chem	47 mm Teflon Filters & PIXE Analysis
Fog Water Chem	Calspan-fab Fog Water Collector & PIXE Analysis
Unactivated Nuclei Chem	Casella Cascade Impactor (& pre-impinger for fog drops) with SEM analysis
Aerosol Size Spectra	PMS 'Knollenberg' aerosol size spectrometers (AFGL instr.)
Liquid Water Content } Mean Drop Size } Drop Concentration }	PMS devices (as above, Models FSSP and ASAS-300)
Fog Water and Dew Deposition	Calspan-fab Dew Scales & Model Meadows
T, T_w, RH	Sling Psychrometers
Temp, Dewpoint Profile	AFGL Instrumentation at Wx Test Facility and at Nobska
Winds	AFGL Instrumentation at Wx Test Facility and at Nobska
Inversion Height	Acoustic Sounder (AFGL instr) at Wx Test Facility
Upper-level Temp/T_d	Chatham Radiosonde; Mini-Sonde (AFGL instr) at Nobska
Trajectory Analysis	AFGL MCIDAS System

Table A-2

GENERAL MEASUREMENTS SCHEDULE

Parameter	Measurement Protocol and Location	
	Nobska Point--Lighthouse	AFGL Wx Test Fac.--Otis AFB
Visibility vs. RH (prediction)	once at ∿1400 EDT	once at ∿1300 EDT (AFGL instr)
Visibility (clear air & lt haze)	continuous at surface level	continuous at surface level
Visibility (dense haze & fog)	continuous at surface level	continuous at 4 hts to 45 m
Total Particle Conc	hourly, ∿1400-0000 EDT	hourly, ∿1300-0000 EDT
CCN/Haze Nuc. Conc	approx. every 4 hr	approx. every 4 hr
Individual Particle Chem	twice: at ∿1400 and 1800 EDT, pre-fog	twice: at ∿1300 and 1800 EDT, pre-fog
Quantitative Aerosol Chem	one 6-8 hr sample, pre-fog	one 6-8 hr sample, pre-fog
Fog Water Chem	one 25 ml sample in mature fog	one 25 ml sample in mature fog
Unactivated Nuclei Chem	one sample in mature fog	one sample in mature fog
Aerosol Size Spectra	means, pre-fog ∿1400 and ∿1800 EDT	means, pre fog ∿1300 and ∿1900 EDT
Liquid Water Content Mean Drop Size Drop Concentration	mean values, mature fog	mean values, mature fog
Fog Water and Dew Deposition	--	hourly
T, Tw, RH	continuous ∿1400-0000 EDT	hourly ∿1300-0000 EDT
Temp, Dewpoint Profile	continuous, at surface level	continuous, at 4 hts to 45 m
Winds	continuous, at surface level	continuous at 4 hts to 45 m
Inversion Height	--	continuous
Meteorological Observations	hourly ∿1300-0000 EDT	hourly ∿1400-0000 EDT
Upper-level Temp/Td	once, daily at ∿1800 EDT	twice daily Chatham Radiosonde
Trajectory Analysis	--	three times daily: 1200, 1700 and 2200 EDT

36

Appendix B
DATA LOGS

Tables B-1 through B-4 present, respectively, the chemical and mass loading data, aerosol and fog droplet concentrations, CCN concentrations, and the aerosol hygroscopicity data. Table B-5 lists the time periods over which the 5 and 60 minute average minimum visibilities were computed for each fog event.

Table B-1

Chemical Composition, Dry Mass Loading (ug/m^3) and Aerosol
Hygroscopicity of the Nobska and Otis Aerosol Samples

SITE	DATE	TIME (EDT) START	STOP	Na	Al	Si	S	Cl	K	Ca	Fe	OTHER	MASS LOADING	HYGROSCOPICITY (M/Mo @ 94%)
OTIS	9 June	925	1730	6	0	8	36	23	9	7	7	4	32.6	
NOBSKA	9 June	1350	2100	16	1	3	6	67	3	3	1	0	47.7	
OTIS	10 June	921	1930	13	6	19	20	16	7	7	9	2	9.2	
NOBSKA	10 June	1315	1945	11	0	6	10	63	3	4	2	0	21.1	
OTIS	11 June	1045	2000	16	0	2	13	60	4	3	2	0	12.1	
NOBSKA	11 June	1345	2010	19	0	1	6	68	3	2	0	0	41.4	
OTIS	12 June	953	2002	21	0	2	11	61	3	2	0	0	15.5	
NOBSKA	12 June	1353	2053	19	0	1	9	66	3	2	1	0	22.5	
OTIS	14 June	1300	2112	18	0	0	72	0	10	0	0	0	9.4	4.6
NOBSKA	14 June	1335	2000	21	0	0	15	57	5	0	0	2	15.0	6.4
OTIS	15 June	1246	2250	3	2	8	68	0	4	3	5	7	40.6	3.4
NOBSKA	15 June	1150	2105	7	0	8	63	0	4	7	6	5	34.6	4.0
OTIS	16 June	945	1946	20	2	9	47	6	7	6	3	1	60.4	3.4
NOBSKA	16 June	1212	2012	14	1	3	10	63	3	4	1	0	68.8	8.6
OTIS	17 June	1127	1952	4	3	12	61	0	9	3	5	3	33.8	3.2
NOBSKA	17 June	1330	1945	18	0	6	44	14	8	5	4	1	34.2	5.0
OTIS	18 June	1141	2051	3	4	17	57	0	6	5	7	2	24.1	3.1
NOBSKA	18 June	1257	2015	9	8	15	51	2	8	4	4	0	14.7	3.9
OTIS	20 June	1230	2030	0	7	22	43	3	9	5	9	3	58.8	1.9
NOBSKA	29 June	1031	2100	15	0	5	20	50	3	3	2	2	24.4	4.8
OTIS	21 June	1118	2002	17	0	4	60	0	7	6	3	2	27.8	4.1
NOBSKA	21 June	1157	1952	21	0	2	35	27	6	5	1	1	23.8	5.1
OTIS	22 June	1152	2003	4	4	18	59	0	4	5	6	0	34.5	3.4
NOBSKA	22 June	1205	2005	9	3	15	55	4	5	5	5	0	72.6	2.9
OTIS	23 June	1245	2015	12	3	16	38	17	6	4	6	0	52.1	2.8
NOBSKA	23 June	1243	2041	18	0	4	24	45	3	4	2	0	37.0	4.7
OTIS	24 June	1115	1945	6	6	26	32	2	8	8	11	1	23.4	2.5
NOBSKA	24 June	1038	2008	16	2	11	24	29	5	7	5	0	31.9	3.6

Table B-2

Summary of the Pre-fog Aerosol and In-fog Droplet
Measurements for the Otis and Nobska Sites

SITE	DATE	SAMPLE TIME START STOP (EDT)		ASAS AITKEN (#/CM3)	.15-3 (#/CM3)	FSSP .5-2.5 (#/CM3)	2.5-47 (#/CM3)	MD (UM)	LWC (G/M3)
OTIS	10 June	1233	1303	1300	126				
NOBSKA	10 June	1442	1517	1200	172				
OTIS	10 June	1931	2001	6000	179				
NOBSKA	10 June	2051	2121	8200	232				
OTIS	11 June	1314	1344	6100	254				
NOBSKA	11 June	1447	1517	3400	959				
NOBSKA	11 June	1843	1913	1050	1037				
OTIS	11 June	2006	2026		847				
OTIS	12 June	1307	1332	11750	342				
NOBSKA	12 June	1458	1509	1800	508				
NOBSKA	12 June	1953	2013	800	563				
OTIS	12 June	2056	2116	3300	519				
OTIS	14 June	1310	1335	3375	634				
NOBSKA	14 June	1436	1501	5800	533				
OTIS	14 June	1937	2002	3700	495				
NOBSKA	14 June	2055	2125	3000	304				
OTIS	15 June	1238	1308	12000	609				
NOBSKA	15 June	1404	1449	3600	1012				
OTIS	15 June	2013	2038	6500	1496				
NOBSKA	15 June	2156	2226	3900	3555	31.5	0.9	4.8	1.11E-04
NOBSKA	15 June	2231	2326	2950	3482	33.5	1.0	4.7	1.14E-04
NOBSKA	15 June	2331	11		3519	33.9	1.2	4.7	1.33E-04
OTIS	16 June	1214	1304	5100	2568				
NOBSKA	16 June	1407	1432	2100	3258				
OTIS	16 June	1927	1952	2650	15923	253.5	16.2	6.7	1.14E-04
NOBSKA	16 June	2051	2126	1550		517.6	295.7	5.9	1.49E-01
NOBSKA	16 June	2131	2226	1600		491.7	388.1	5.2	1.29E-01
NOBSKA	16 June	2231	2251	1500		570.6	300.0	4.9	7.05E-02

SITE	DATE	SAMPLE TIME START STOP (EDT)		AITKEN (#/CM3)	ASAS .15-3 (#/CM3)	FSSP .5-2.5 (#/CM3)	2.5-47 (#/CM3)	MD (UM)	LWC (G/M3)
OTIS	17 June	1240	1310	3100	3272				
NOBSKA	17 June	1407	1452	3500	4112	79.9	5.2	4.7	6.21E-04
NOBSKA	17 June	1808	1813	6050	533				
OTIS	17 June	1910	1935	2500	476				
OTIS	18 June	1231	1311	12000					
NOBSKA	18 June	1406	1446	4000	2317				
NOBSKA	18 June	1808	1828	2700					
NOBSKA	18 June	1853	1923	2900					
NOBSKA	18 June	1948	2028	2350	1552				
NOBSKA	18 June	2048	2128	2500		278.5	248.3	8.3	3.66E-01
NOBSKA	18 June	2133	2218	2100		257.8	252.6	10.1	6.26E-01
OTIS	18 June	2311	2346	7000		189.8	70.8	14.4	2.16E-01
OTIS	19 June	1235	1300	2000	3286	67.1	8.2	9.5	3.18E-04
OTIS	20 June	1311	1336	46000	265				
NOBSKA	20 June	1423	1449	14500	240				
NOBSKA	20 June	2028	2058	11000	527				
OTIS	20 June	2144	2209	23000	552				
OTIS	21 June	1144	1209	11000	492				
NOBSKA	21 June	1255	1300	2900	520				
NOBSKA	21 June	1339	1404	4300	837				
NOBSKA	21 June	1916	2041	3400	1742				
OTIS	21 June	2129	2154	6000	2272				
OTIS	22 June	1252	1317	55000	529				
NOBSKA	22 June	1408	1443	10800	708				
NOBSKA	22 June	1944	2024	19500	1987				
NOBSKA	22 June	2331	2356	1400		380.1	42.6	5.6	1.49E-02
OTIS	23 June	52	117	2700		437.7	9.5	5.2	4.18E-03
OTIS	23 June	1257	1327	10000	567				
NOBSKA	23 June	1450	1515	5300	740				
NOBSKA	23 June	1934	2004	6700	914				
OTIS	23 June	2053	2123	15000	954				
OTIS	24 June	1227	1257	28500	108				
NOBSKA	24 June	1445	1500	9100	396				
NOBSKA	24 June	1941	2006	9500	749				
OTIS	24 June	2057	2132	10800	785				

Table B-3

Cloud Condensation Nuclei (CCN) Spectra

SITE	DATE	(EDT) TIME	CCN CONCENTRATION (#/CM3) FOR INDICATED SUPERSATURATION			
			0.1%	0.2%	0.5%	1.0%
OTIS	6 June	1610	187	250	367	660
OTIS	7 June	1155	66	95	153	218
OT'S	8 June	1235	219	460	1230	2570
OTIS	9 June	908	216	304	470	660
NOBSKA	9 June	1630	18	71	455	1910
OTIS	10 June	1040	219	330	580	880
NOBSKA	10 June	1520	103	163	302	488
NOBSKA	10 June	1920	158	280	600	1060
OTIS	11 June	1440	288	353	470	585
NOBSKA	11 June	1443	149	177	222	433
OTIS	11 June	1856	205	238	293	340
NOBSKA	11 June	1920	225	258	312	360
OTIS	12 June	1000	245	260	284	305
OTIS	12 June	1535	263	282	312	337
NOBSKA	12 June	1440	88	124	197	282
OTIS	12 June	2030	255	279	315	348
NOBSKA	12 June	2027	137	196	312	447
OTIS	13 June	1301	255	290	350	400
NOBSKA	13 June	1604	140	179	249	322
OTIS	14 June	1122	365	423	520	615
OTIS	14 June	1435	740	1180	2200	3500
NOBSKA	14 June	1502	87	129	219	326
OTIS	14 June	1956	395	675	1385	2400
NOBSKA	14 June	2010	49	97	236	467
OTIS	15 June	1325	388	430	500	555
NOBSKA	15 June	1423	430	668	1205	1885
OTIS	15 June	1640	625	950	1230	1750
NOBSKA	15 June	1656	725	1130	2020	3170
OTIS	15 June	2103	845	1150	1730	2370
NOBSKA	15 June	2030	1380	1900	2940	4090
OTIS	16 June	958	890	1140	1580	2040
OTIS	16 June	1255	1100	1450	2080	2770
NOBSKA	16 June	1255	660	890	1340	1330
OTIS	16 June	1950	630	940	1650	2530
NOBSKA	16 June	1958	454	610	915	1240
OTIS	16 June	2310	507	670	970	1290
NOBSKA	16 June	2221	413	517	755	985

41

Table B-3(continued)

SITE	DATE	(EDT) TIME	CCN CONCENTRATION (#/CM3) FOR INDICATED SUPERSATURATION			
			0.1%	0.2%	0.5%	1.0%
OTIS	17 June	1135	680	910	1340	1800
OTIS	17 June	1320	560	635	915	1135
NOBSKA	17 June	1437	520	808	1460	2300
OTIS	17 June	1846	468	575	760	935
NOBSKA	17 June	1850	378	505	743	1000
OTIS	18 June	1202	440	610	930	1290
OTIS	18 June	1409	470	805	1650	2840
NOBSKA	18 June	1315	154	306	760	1520
OTIS	18 June	1856	515	785	1380	2120
NOBSKA	18 June	1900	212	375	800	1440
OTIS	18 June	2240	234	279	465	1830
NOBSKA	18 June	2240	111	193	400	700
OTIS	19 June	1333	265	312	440	1070
NOBSKA	19 June	1356	141	213	370	565
OTIS	20 June	1325	350	540	965	1500
NOBSKA	20 June	1249	242	304	420	535
OTIS	20 June	2113	795	990	1310	1640
NOBSKA	20 June	2125	433	486	570	645
OTIS	21 June	1357	630	910	1460	2100
OTIS	21 June	1451	387	670	1370	2400
NOBSKA	21 June	1355	355	600	1240	2100
OTIS	21 June	2030	595	965	1850	3050
NOBSKA	21 June	2021	416	668	1240	2000
OTIS	22 June	1347	720	940	1340	1775
NOBSKA	22 June	1330	570	915	1700	2760
OTIS	22 June	2050	705	1010	1625	2350
NOBSKA	22 June	2051	475	680	1075	1540
NOBSKA	22 June	2311	473	573	742	900
OTIS	23 June	1334	646	920	1460	2100
NOBSKA	23 June	1340	360	600	1185	200
OTIS	23 June	2026	625	895	1450	2100
NOBSKA	23 June	2028	449	646	1060	1540
OTIS	24 June	1255	268	415	745	1160
NOBSKA	24 June	1238	212	414	1005	2000
OTIS	24 June	2000	605	1140	2650	5050
NOBSKA	24 June	2044	600	1050	2230	3950

Table B-4.

Hygroscopicity (M/M_o) of the Nobska and Otis aerosol at various relative humdities.

		HYGROSCOPICITY (M/Mo) @ RH=				
SITE	DATE	71%	78%	89%	94%	98%
OTIS	14 JUNE	1.50	1.90	2.90	4.60	26.60
NOBSKA	14 JUNE	1.84	2.26	3.60	6.40	34.40
OTIS	15 JUNE	1.30	1.60	2.22	3.40	12.95
NOBSKA	15 JUNE	1.45	1.66	2.41	3.97	15.50
OTIS	16 JUNE	1.36	1.65	2.29	3.40	12.20
NOBSKA	16 JUNE	2.35	2.98	4.91	8.64	23.60
OTIS	17 JUNE	1.32	1.56	2.12	3.20	14.10
NOBSKA	17 JUNE	1.51	1.31	2.79	4.95	25.40
OTIS	18 JUNE	1.21	1.52	2.06	3.96	14.50
NOBSKA	18 JUNE	1.41	1.64	2.32	3.91	28.95

		HYGROSCOPICITY (M/Mo) @ RH=				
SITE	DATE	66%	79%	84%	94%	98%
OTIS	20 JUNE	1.06	1.19	1.29	1.86	6.70
NOPSKA	20 JUNE	1.38	2.00	2.37	4.83	14.80
OTIS	21 JUNE	1.27	1.69	2.00	4.09	16.00
NOBSKA	21 JUNE	1.43	2.13	2.50	5.10	18.70
OTIS	22 JUNE	1.08	1.54	1.70	3.35	14.80
NOBSKA	22 JUNE	1.20	1.47	1.65	2.88	9.98
OTIS	23 JUNE	1.09	1.42	1.62	2.85	10.50
NOBSKA	23 JUNE	1.26	2.00	2.42	4.70	14.40
OTIS	24 JUNE	1.08	1.32	1.44	2.48	13.40
NOBSKA	24 JUNE	1.25	1.65	1.91	3.56	10.60

Table B-5

Time periods of 5 and 60 minute average minimum visibilities for evaluated fog episodes.

SITE	DATE	AVERAGE MINIMUM VISIBILITY					
		60min VSBY	TIME (EDT)	DAY	5min VSBY	TIME (EDT)	DAY
OTIS	16-17 JUNE	302m	2033-2133	6/16	271m	2048	6/16
NOBSKA	16-17 JUNE	77m	2043-2143	6/16	72m	2103	6/16
NOBSKA	18 JUNE	114m	0938-1038	6/18	86m	1028	6/18
OTIS	18-19 JUNE	160m	0428-0528	6/19	138m	0353	6/19
NOBSKA	18-19 JUNE	61m	2108-2208	6/18	45m	2143	6/18
OTIS	22 JUNE	139m	0403-0503	6/22	93m	0503	6/22
OTIS	22-23 JUNE	250m	0233-0333	6/23	210m	0018	6/23
NOBSKA	22-23 JUNE	139m	0438-0538	6/23	108m	0443	6/23

Appendix C
EXAMPLES OF MCIDAS STREAMLINE PATTERN CLASSIFICATIONS

Figures C-1 through C-5 present an example of the MCIDAS streamline pattern for each of the five flow classifications: marine, primarily marine, mixed, primarily continental and continental.

SFC STR   131600
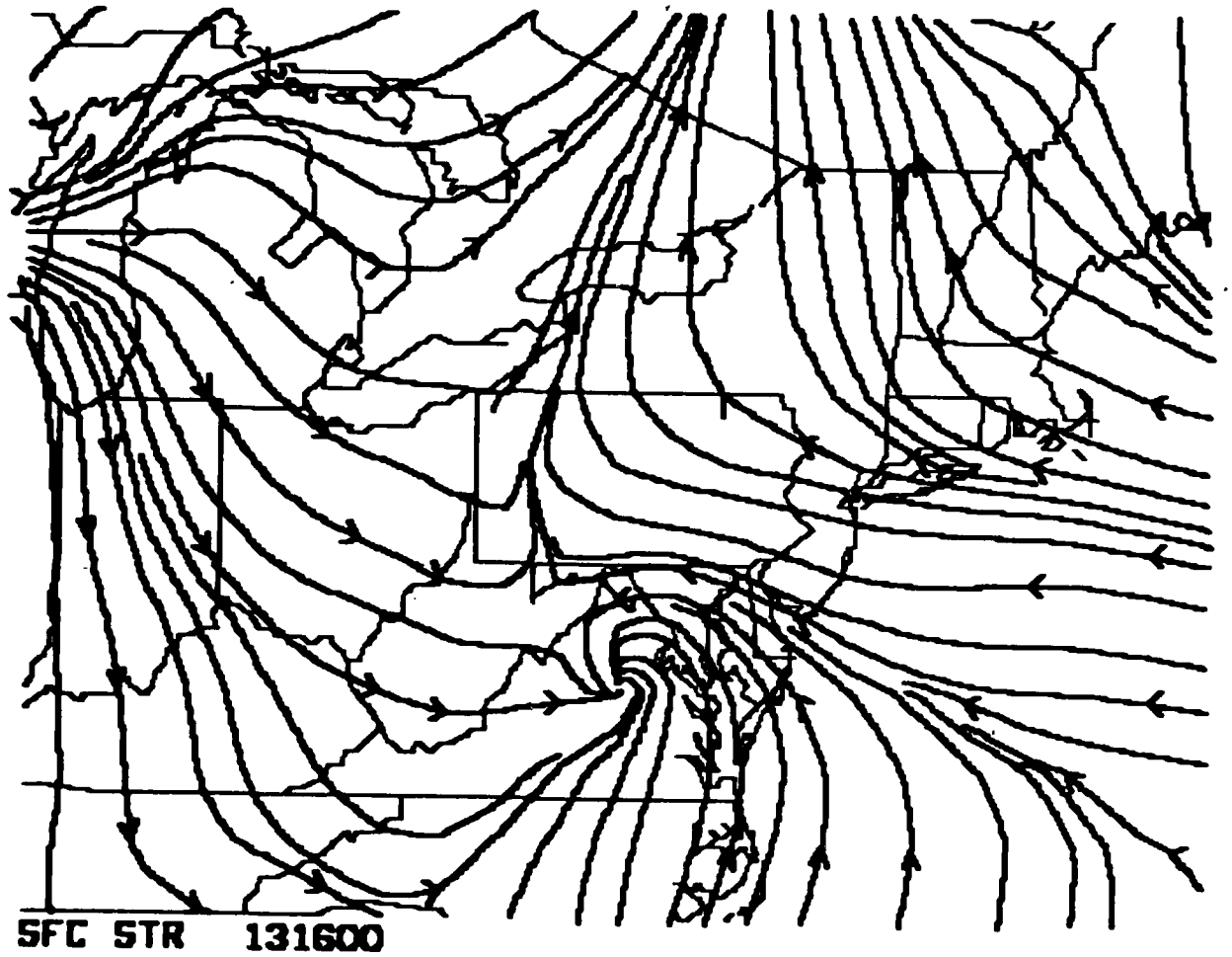
Figure C-1. An example of a MARINE flow pattern.

46

SFC STR   210200
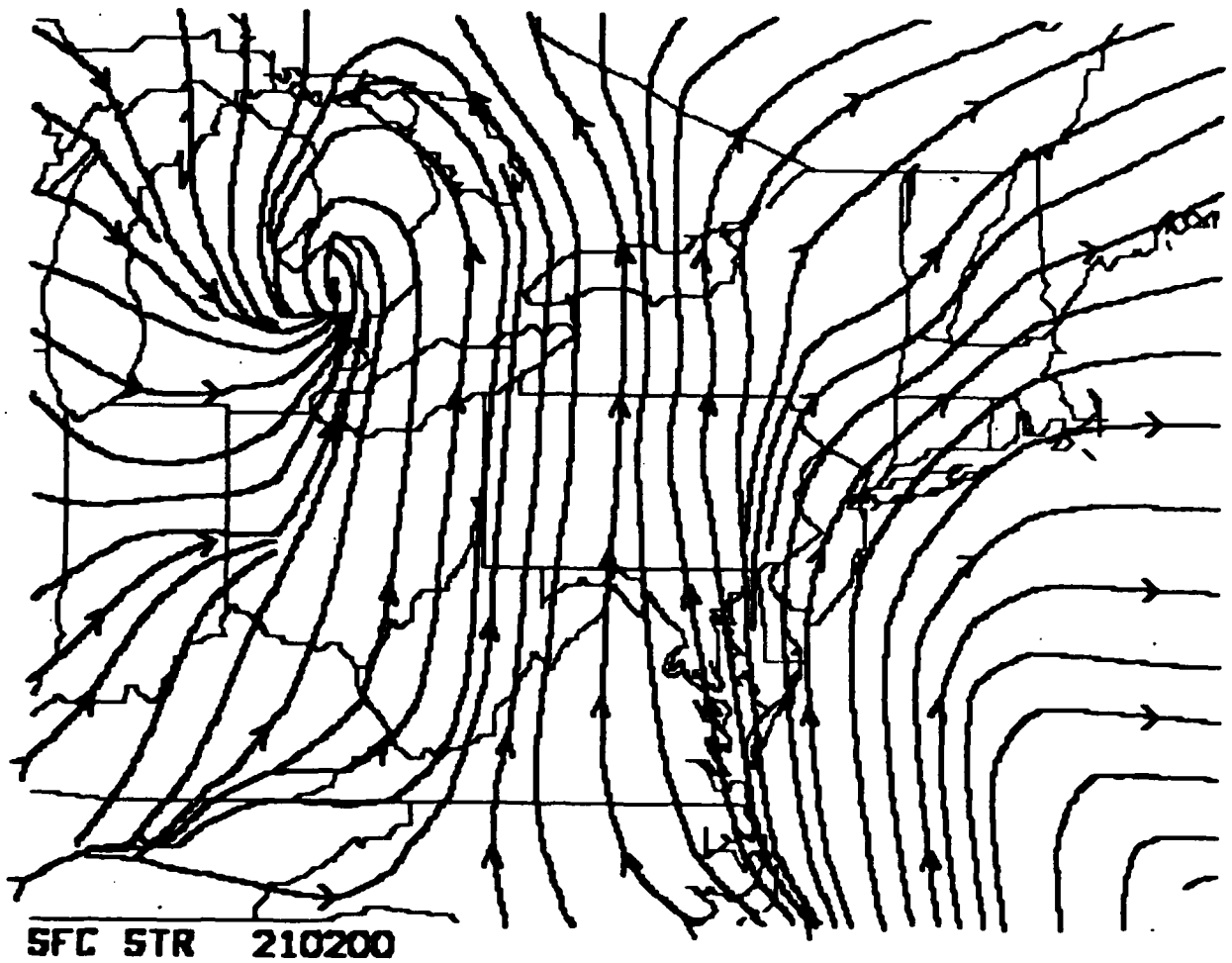
Figure C-2. An example of a PRIMARILY MARINE flow pattern.

47

SFC STR   161600
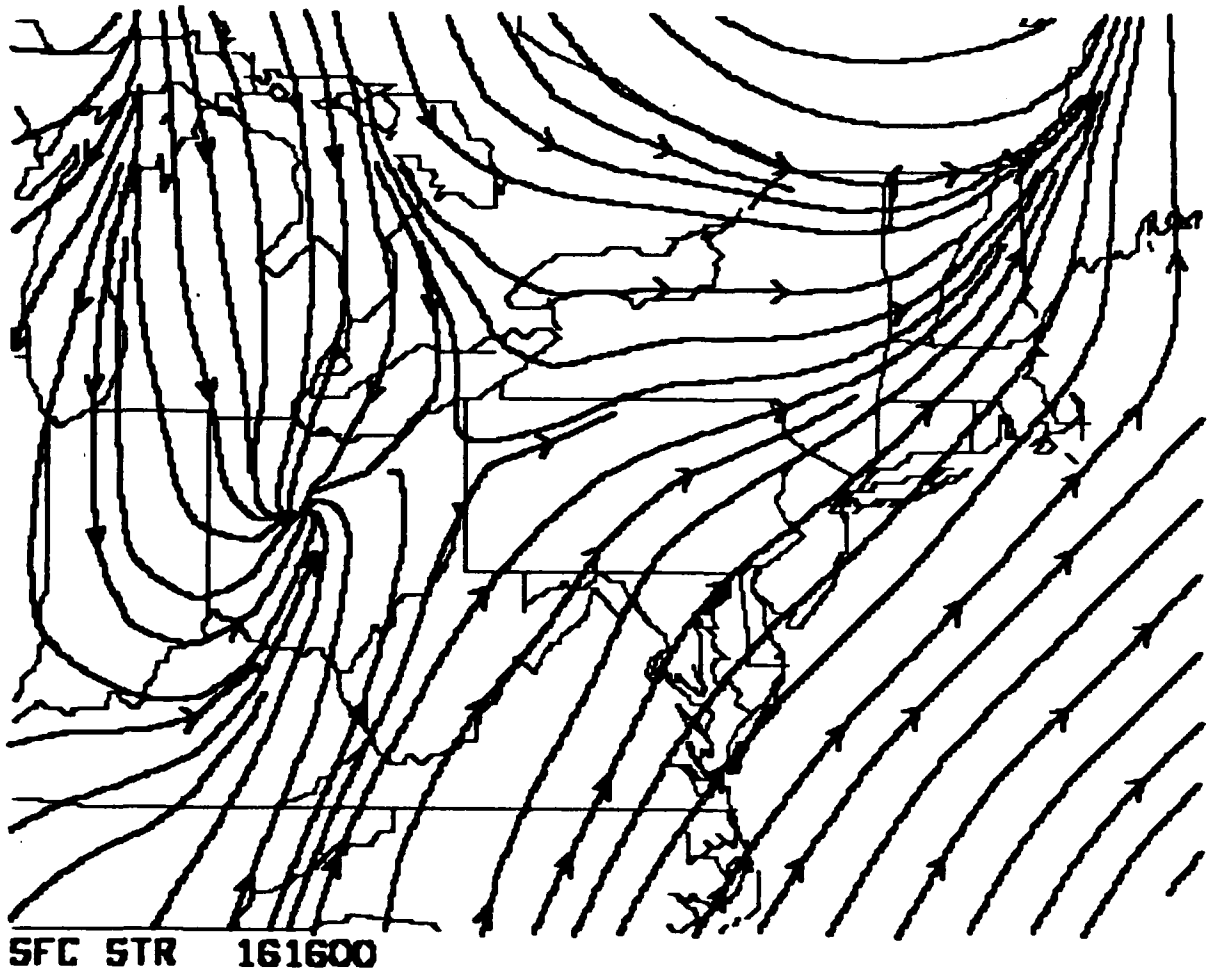
Figure C-3. An example of a MIXED flow pattern.

48

SFC STR   171600
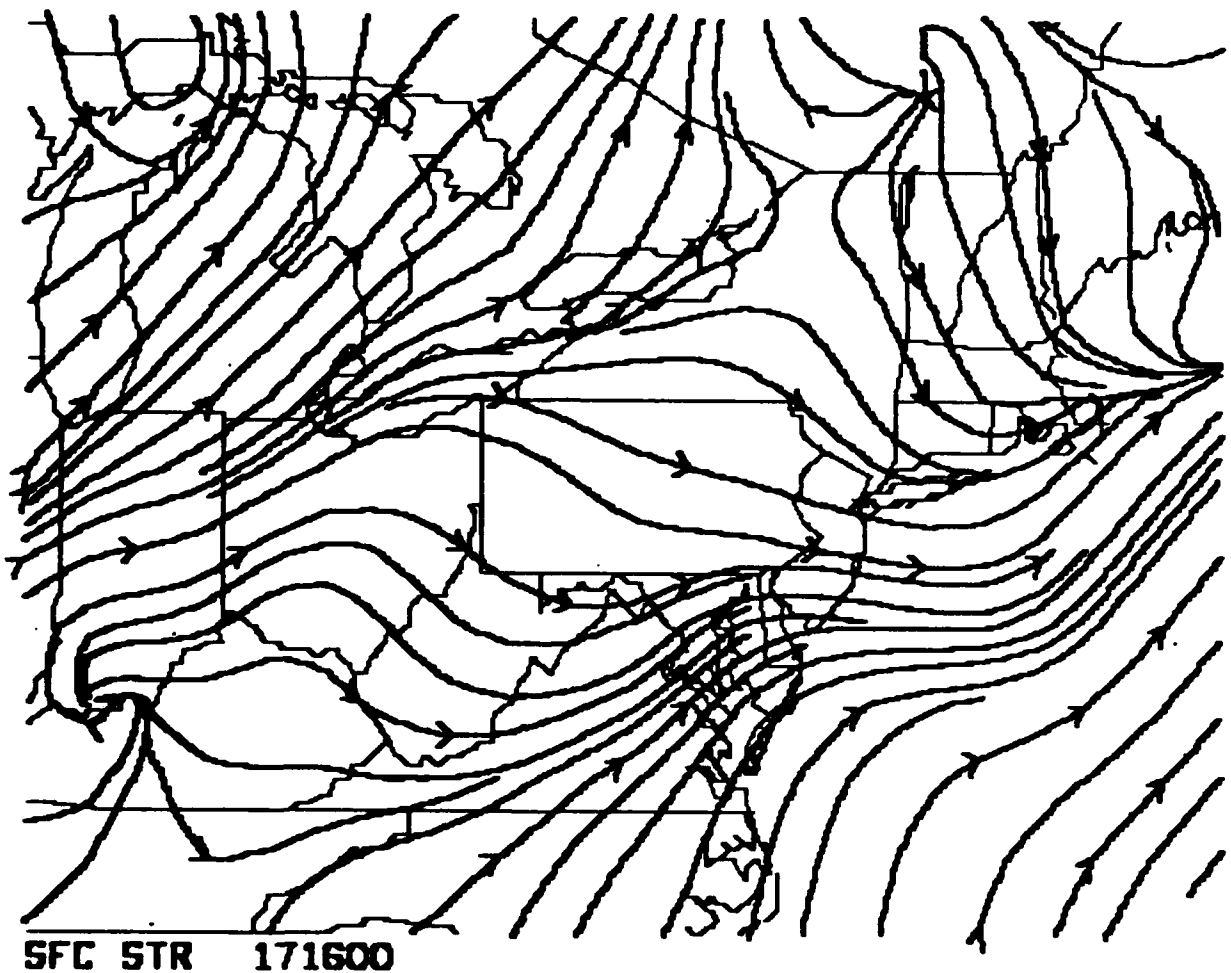
Figure C-4. An example of a PRIMARILY CONTINENTAL flow pattern.

SFC STR 240200
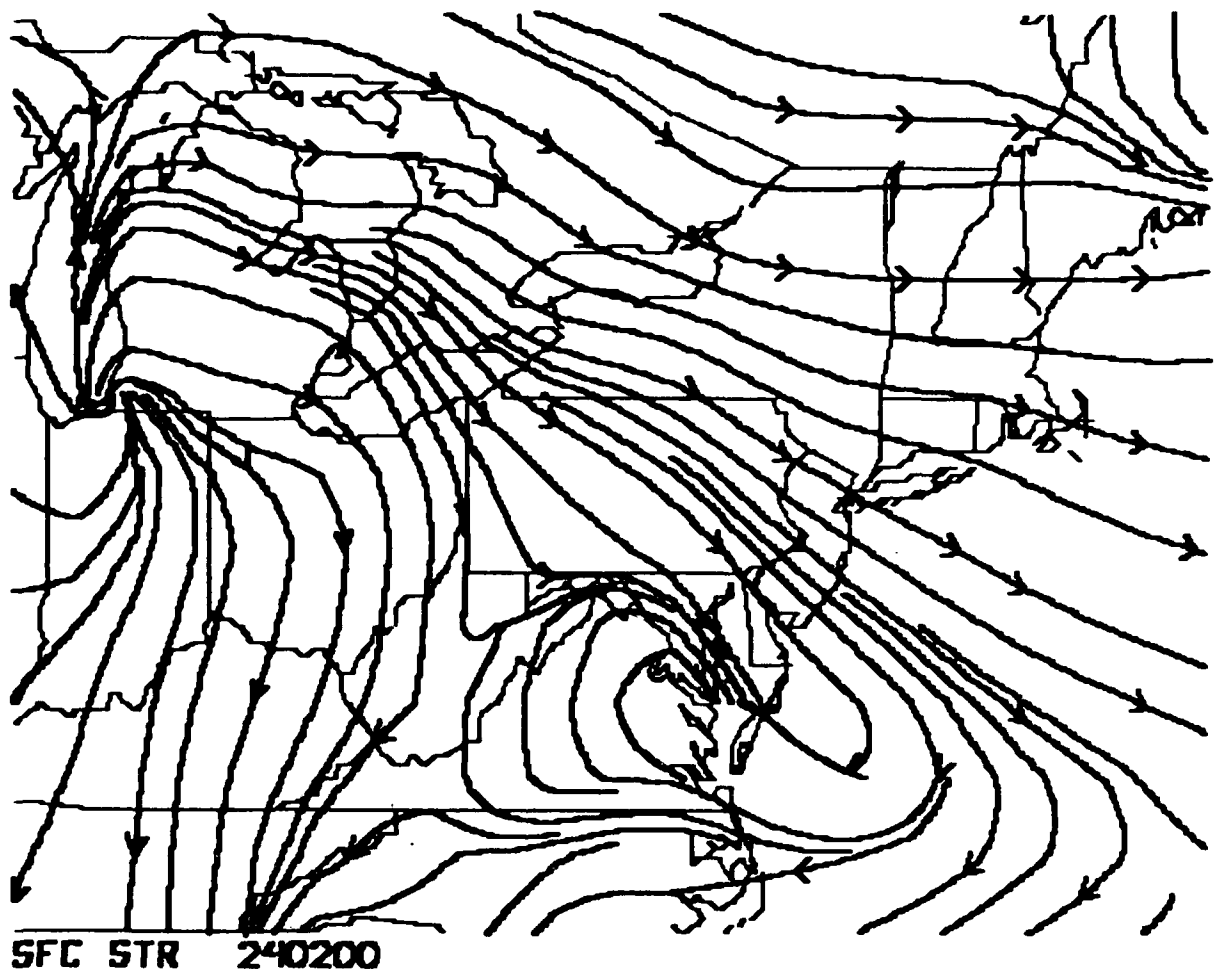
Figure C-5. An example of a CONTINENTAL flow pattern.

Appendix D
PLOTS OF VISIBILITY, RELATIVE HUMIDITY, WIND SPEED
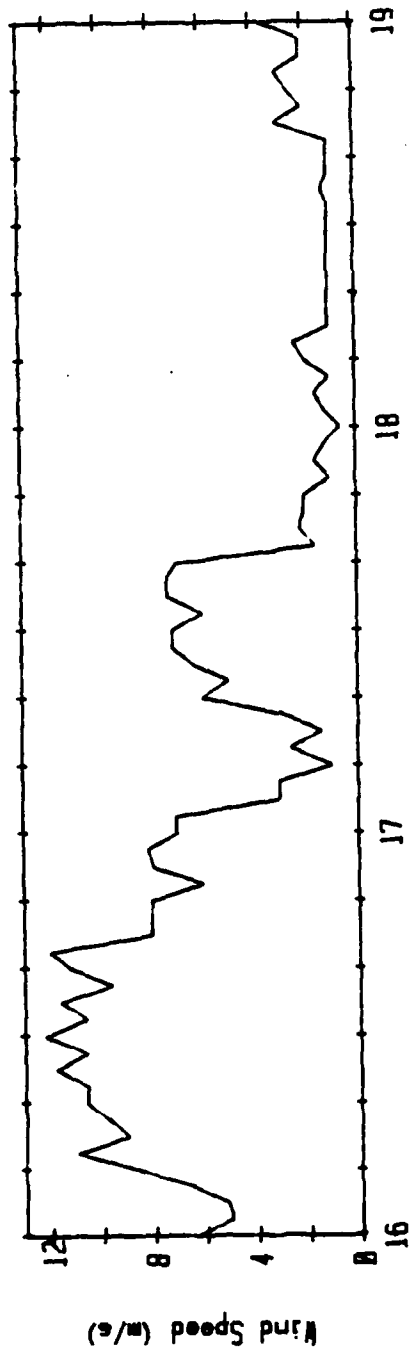## AND WIND DIRECTION AS FUNCTIONS OF TIME AT THE
OTIS AFB SITE.

Key: dotted line = relative humidity data

solid bar = acquisition period of precursor aerosol filter sample.

A = time of aerosol size distribution measurement with the PMS ASAS probe.

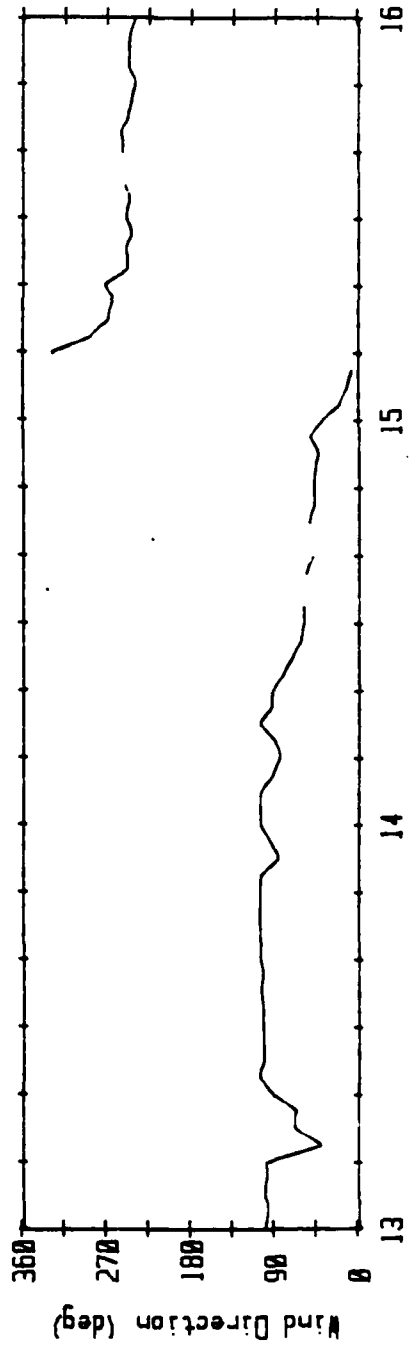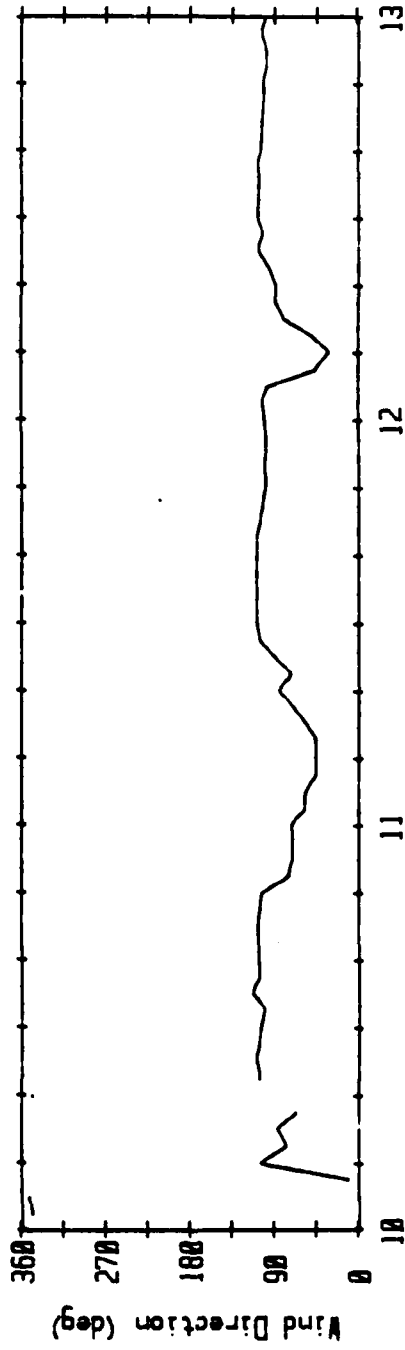F = time of aerosol size distribution measurement with the PMS FSSP probe.

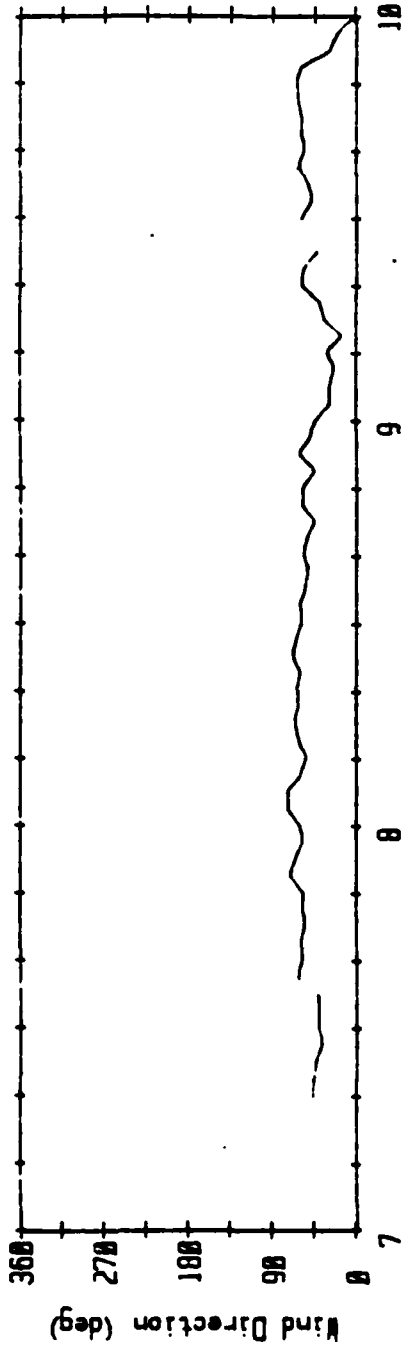C = time of CCN concentration measurement.

Date in June (local time)

52

Date in June (local time)

53

Date in June (local time)

54

Date in June (local time)

55

Wind Direction (deg)

Date in June (local time)

Date in June (local time)

57
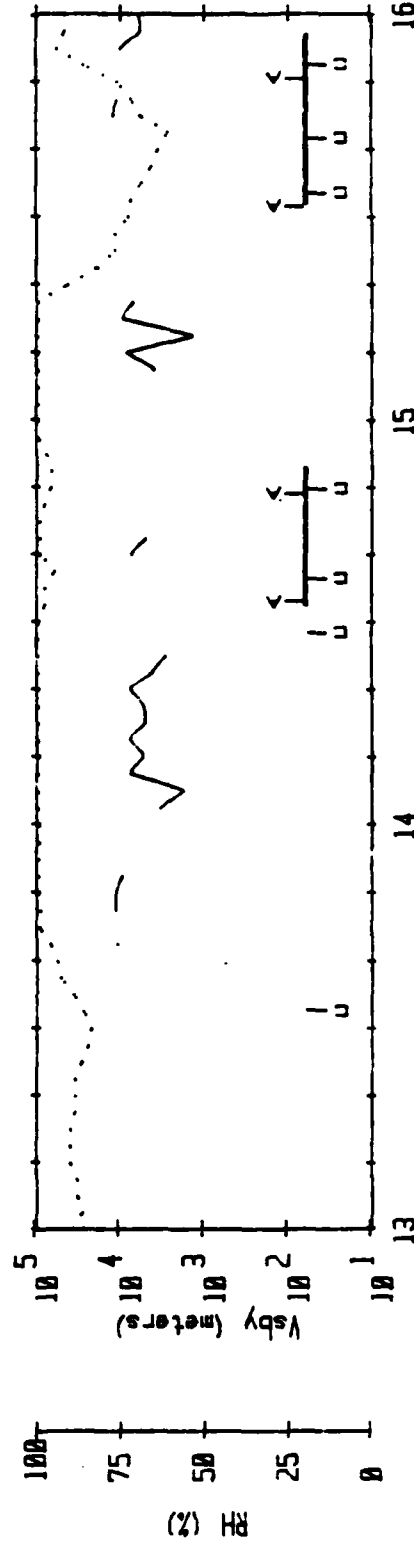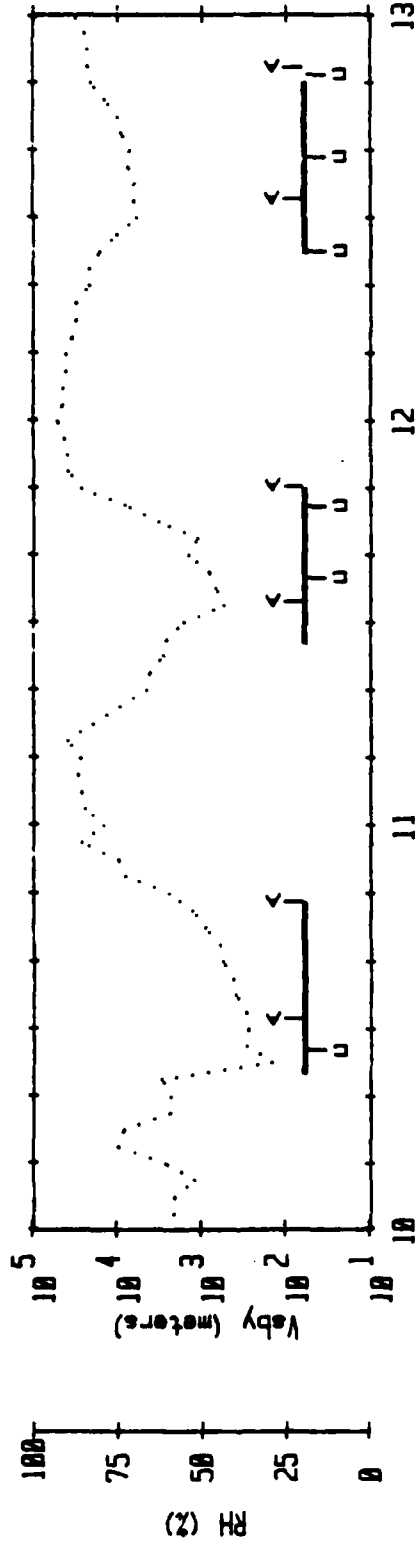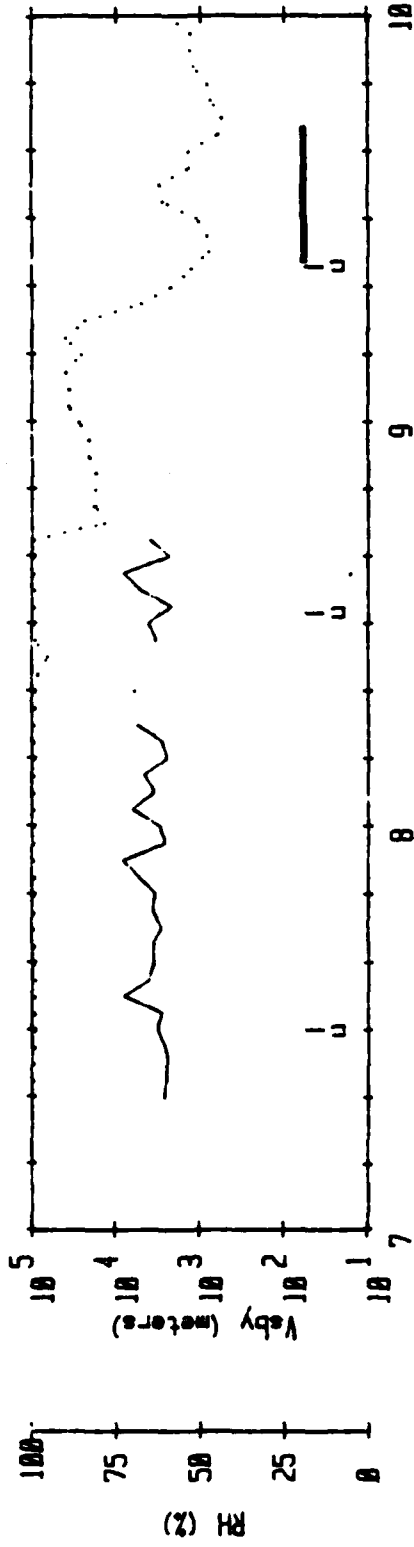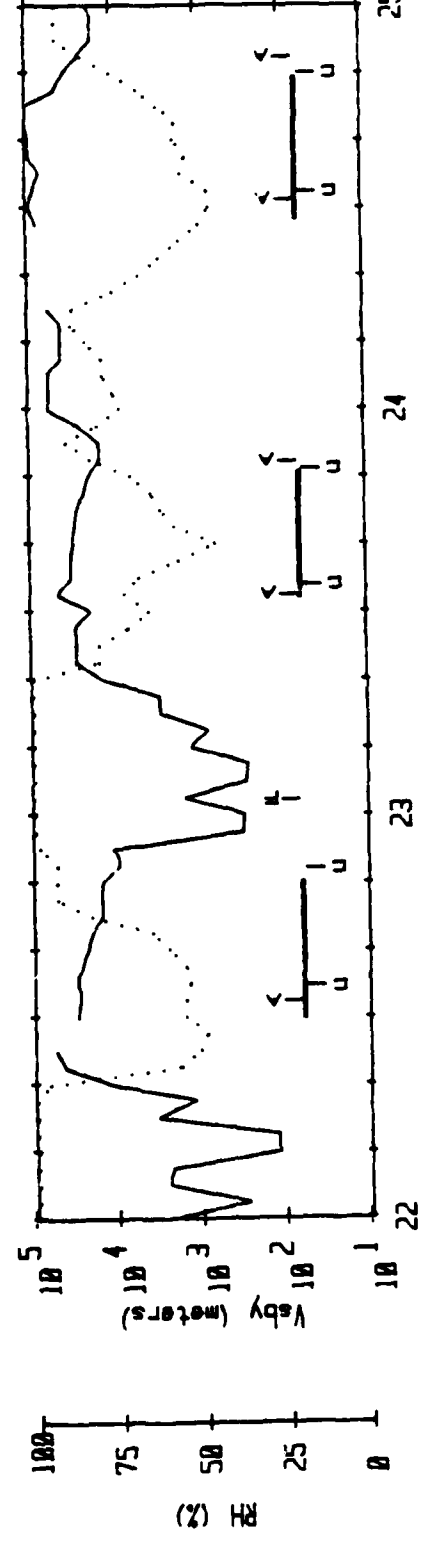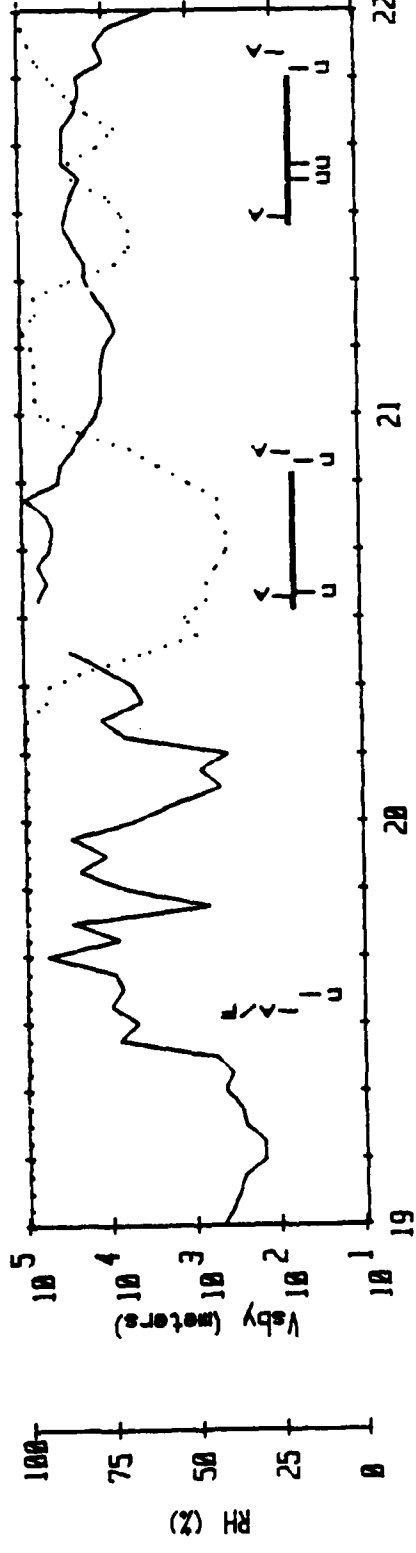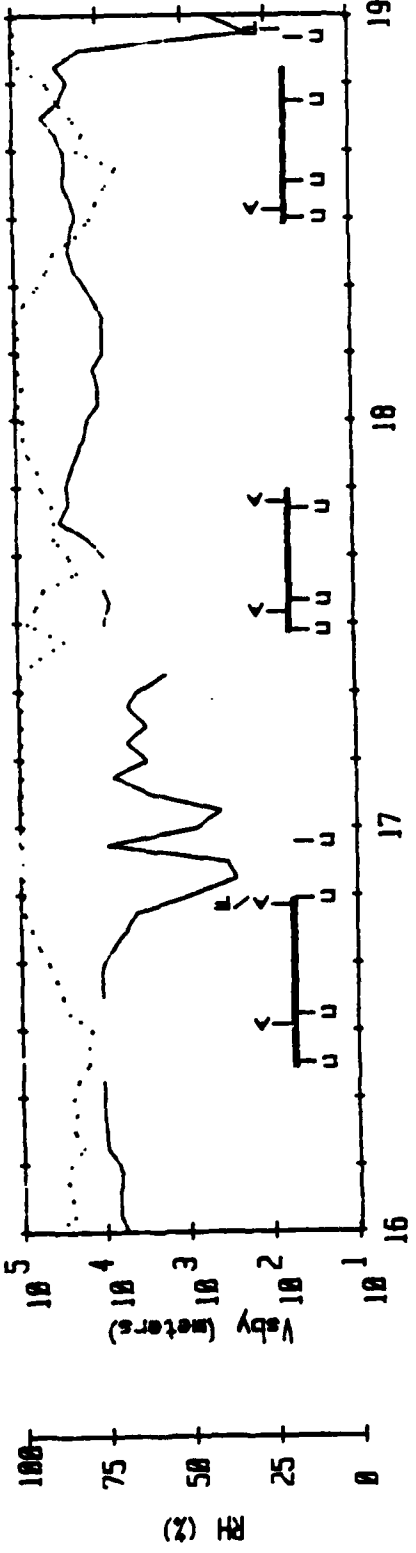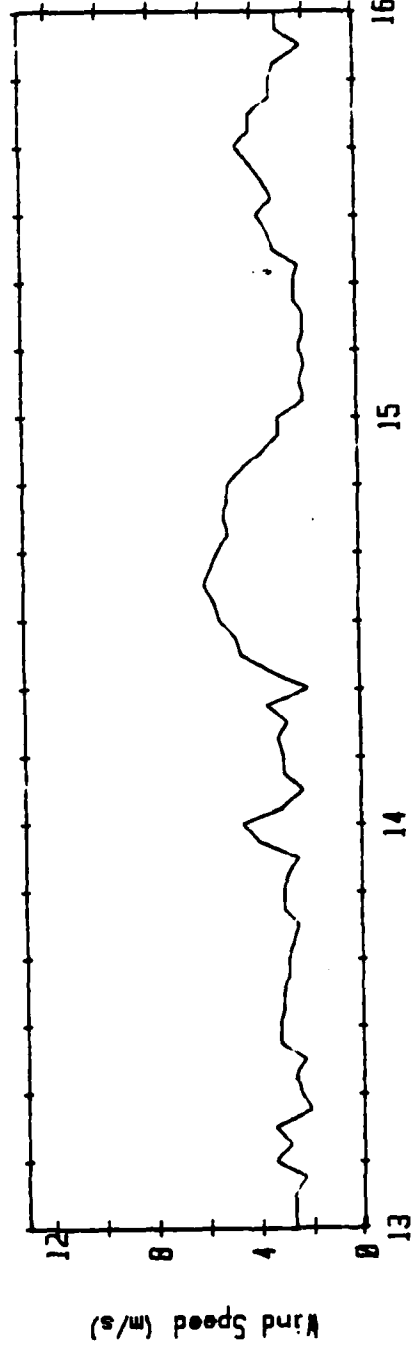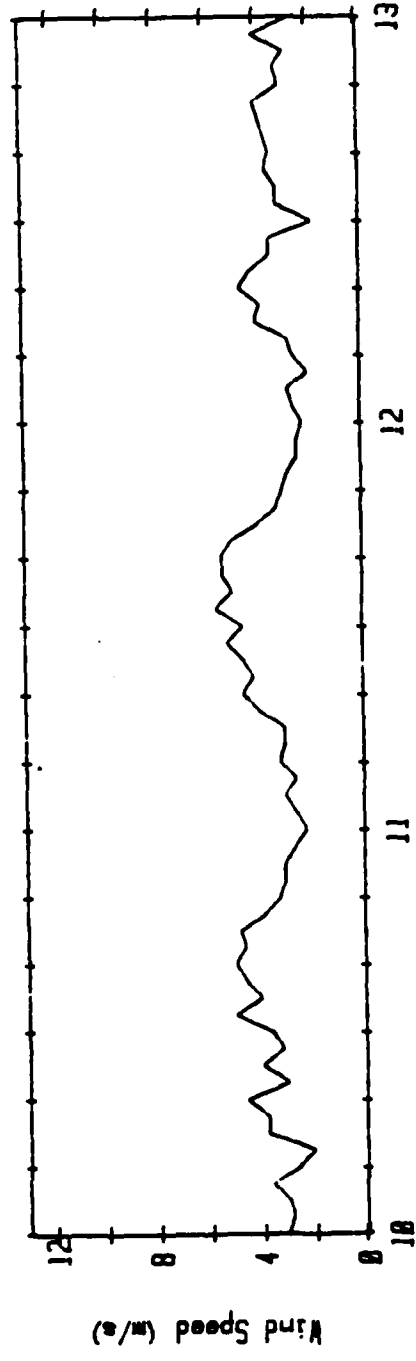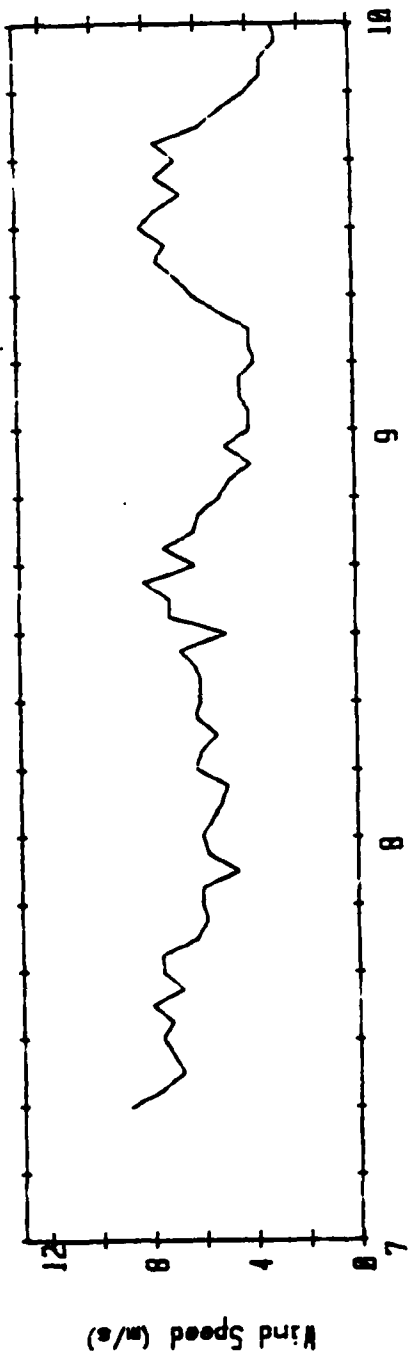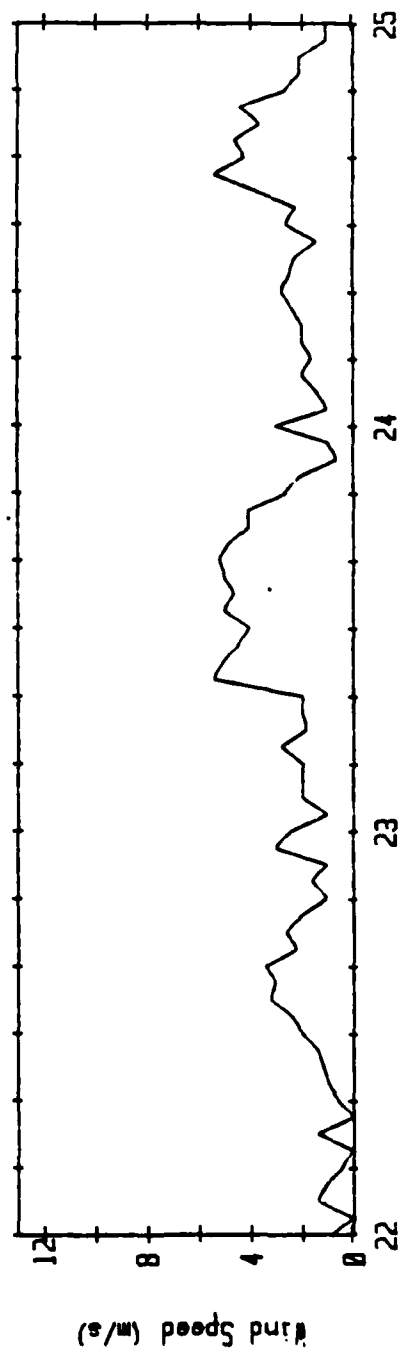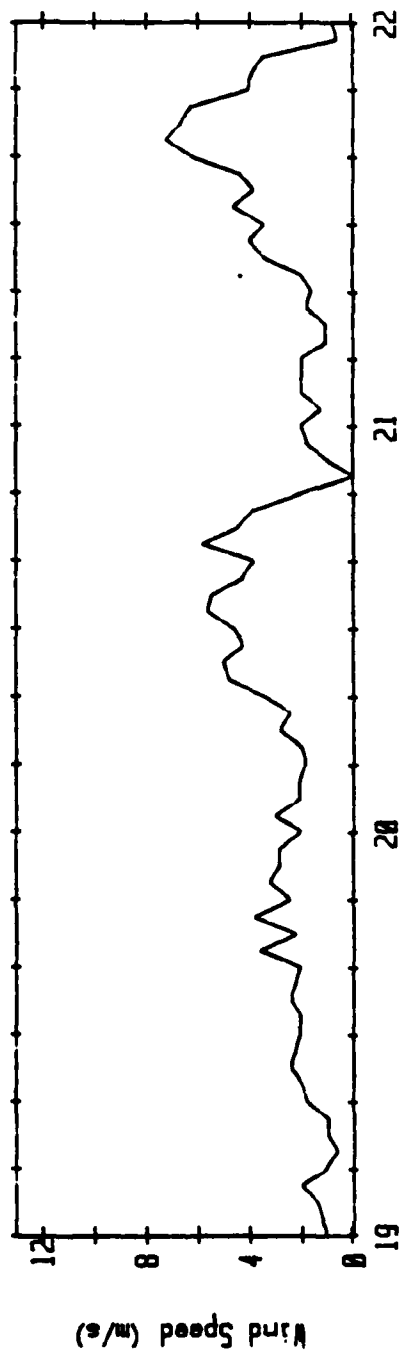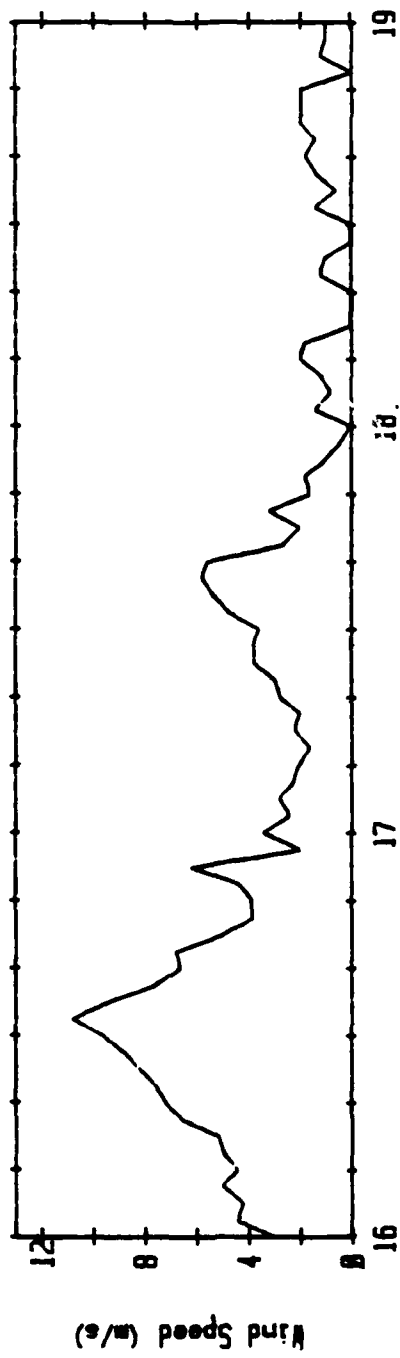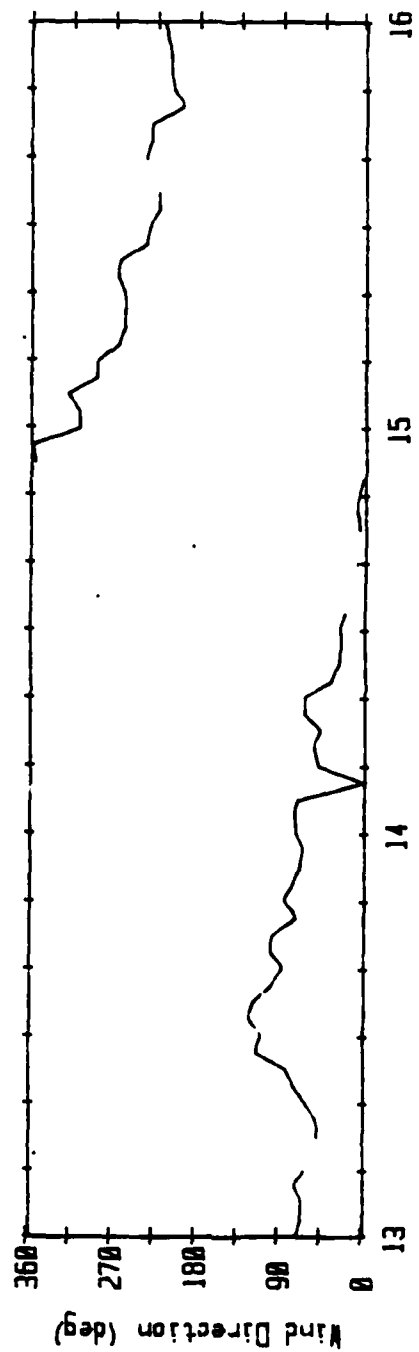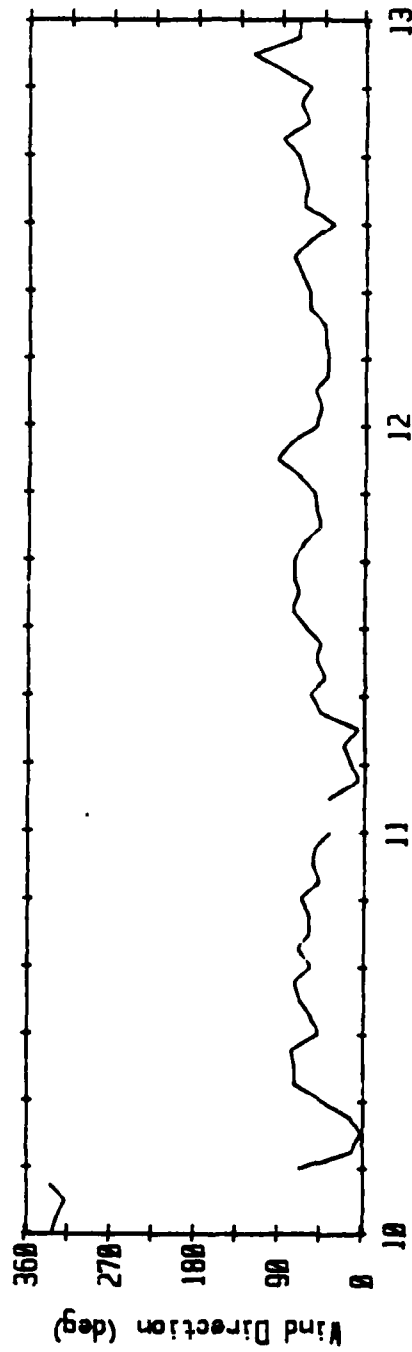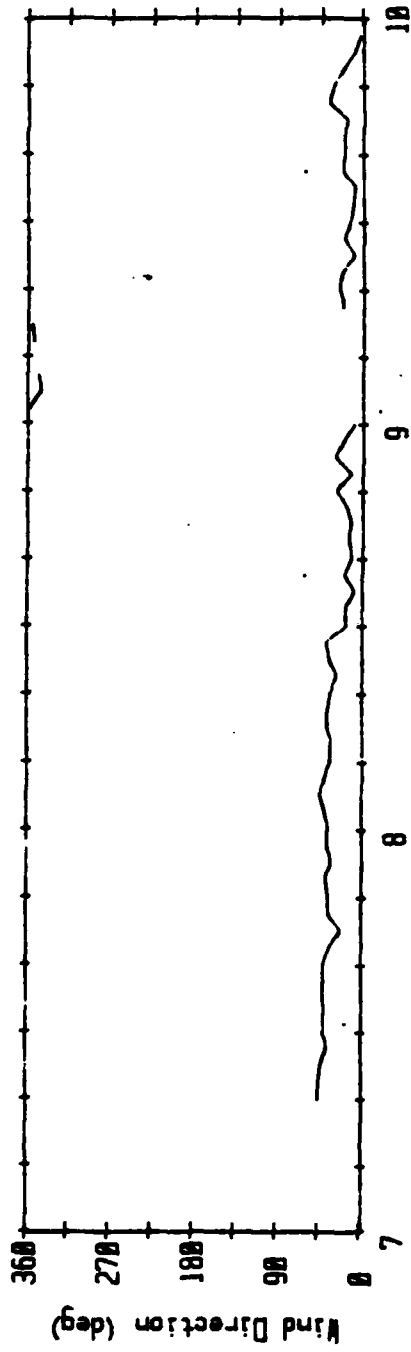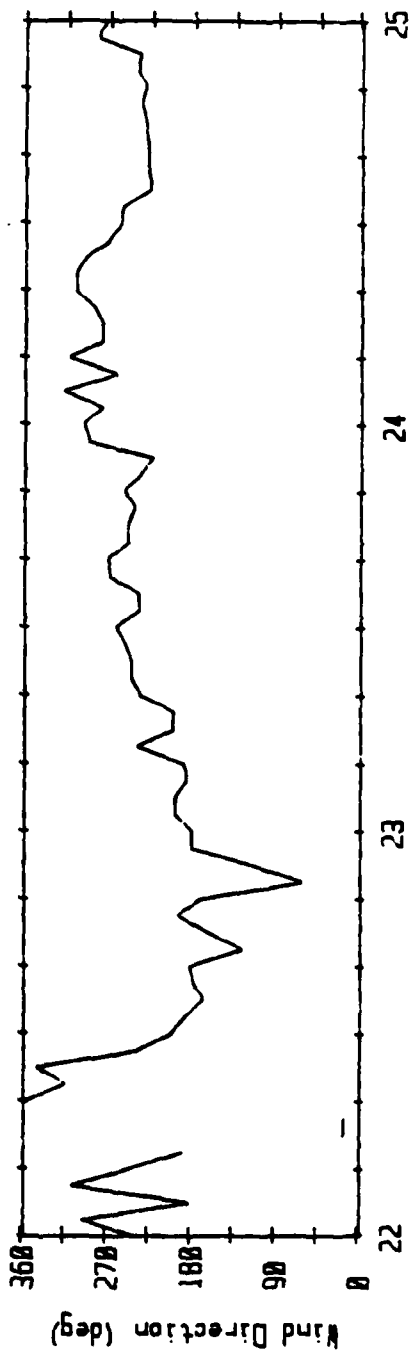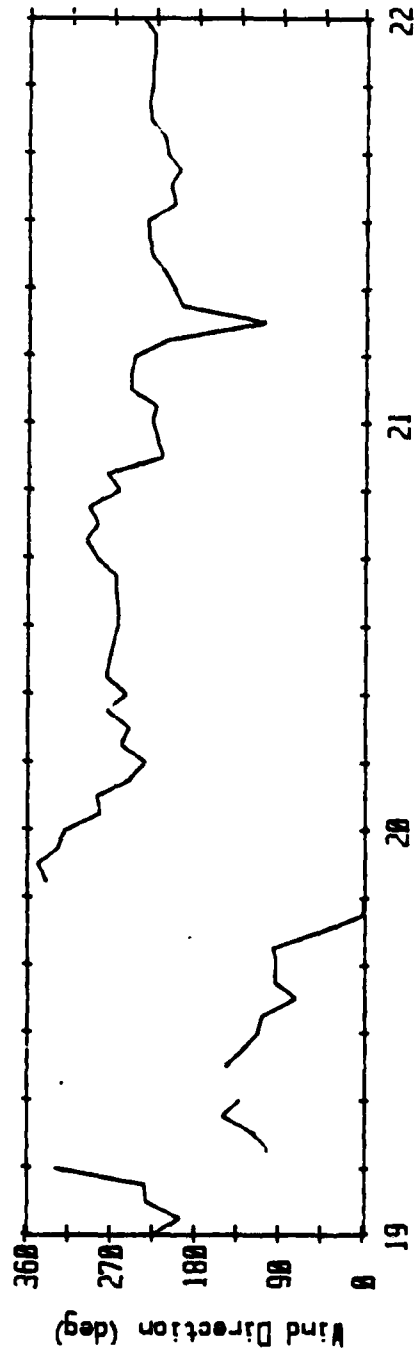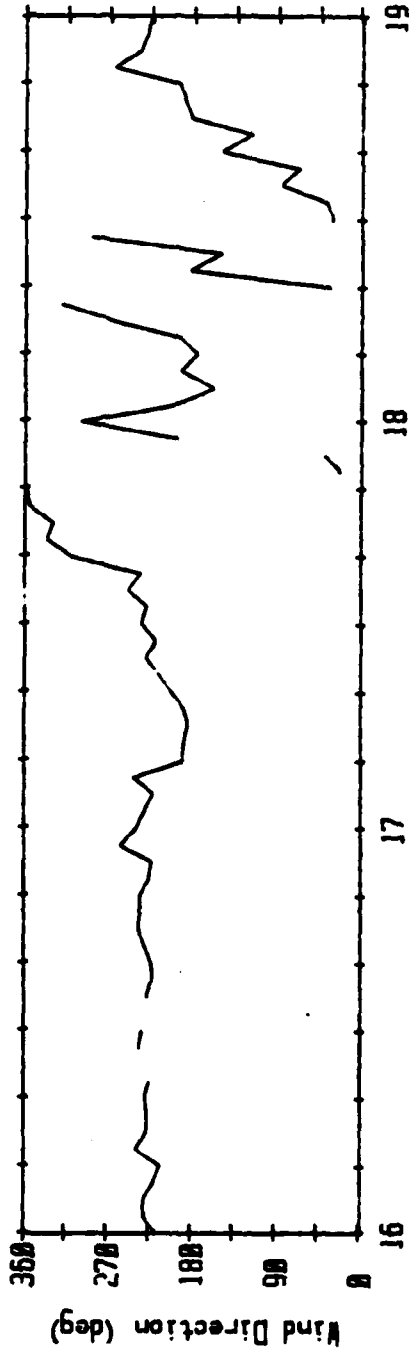
Appendix E
PLOTS OF VISIBILITY, RELATIVE HUMIDITY, WIND SPEED
AND WIND DIRECTION AS FUNCTIONS OF TIME AT
THE NOBSKA SITE

Key: dotted line = relative humidity data

solid bar = acquisition period of precursor aerosol filter sample

A = time of aerosol size distribution measurement with the PMS ASAS probe

F = time of aerosol size distribution measurement with the PMS FSSP probe

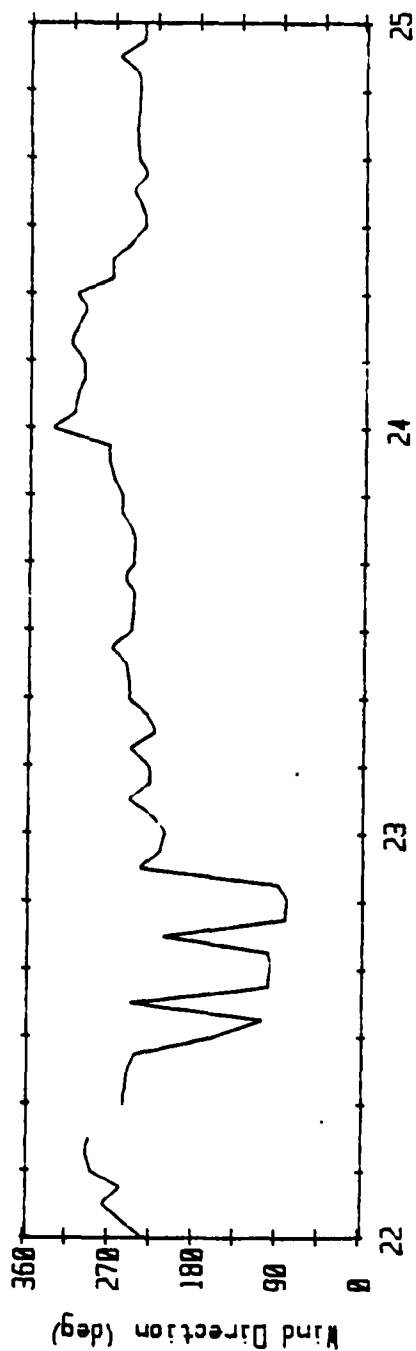C = time of CCN concentration measurement.

Date in June (local time)

Date in June (local time)

360 270 180 90 0
Wind Direction (deg)

360 270 180 90 0
Wind Direction (deg)

360 270 180 90 0
Wind Direction (deg)

16   17   18   19

19   20   21   22

22   23   24   25
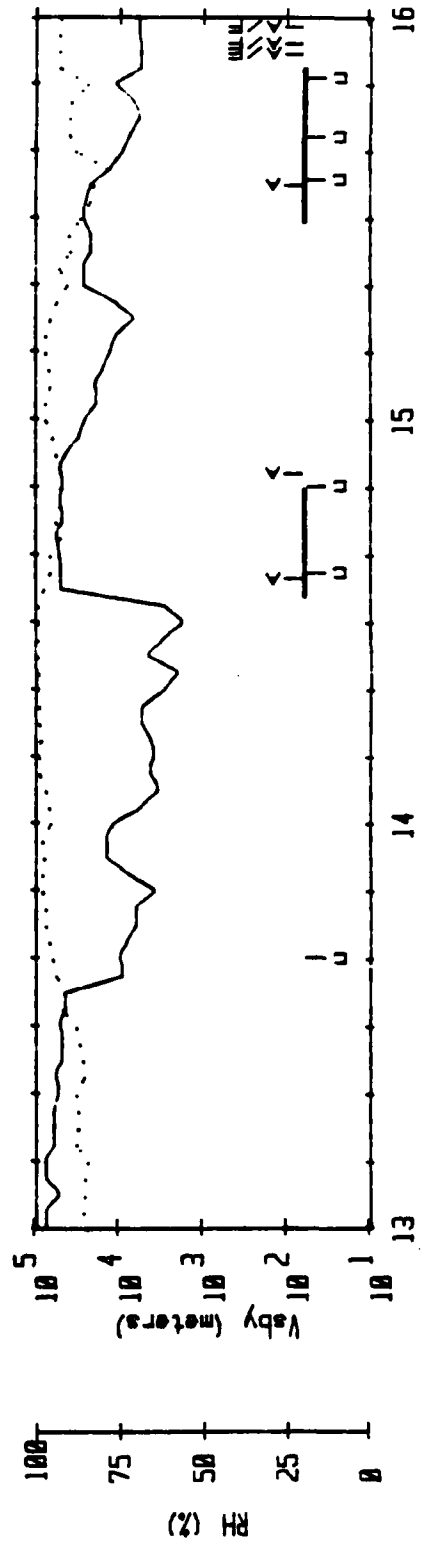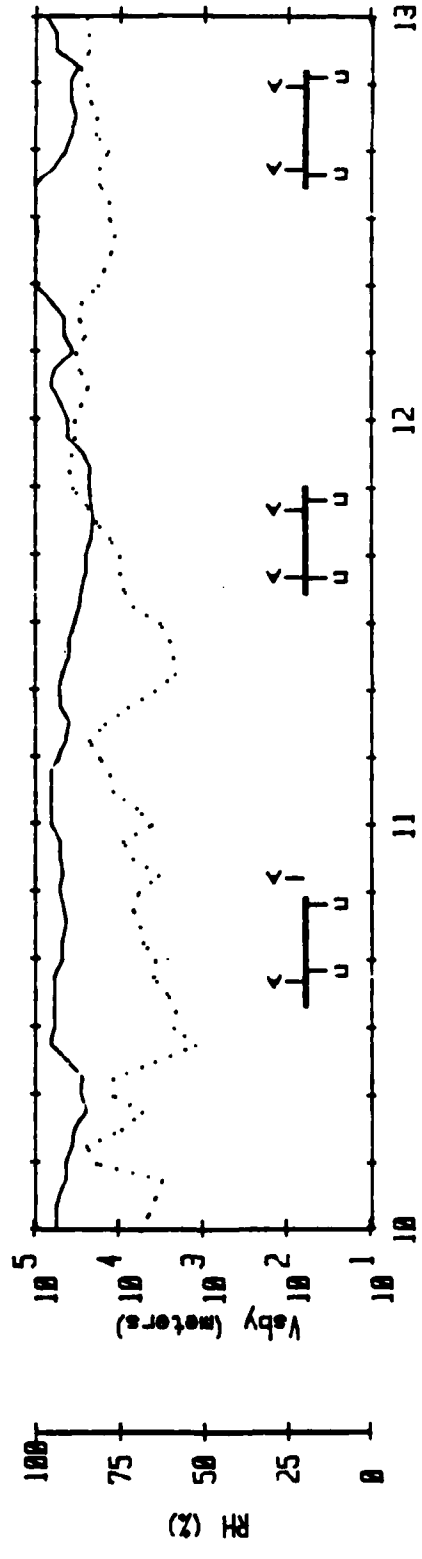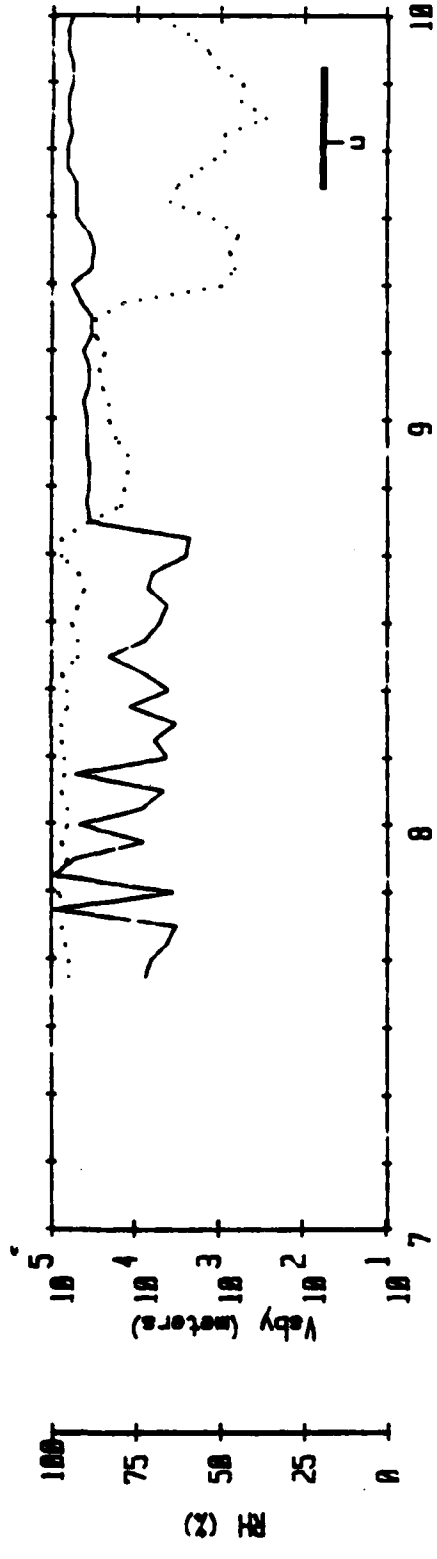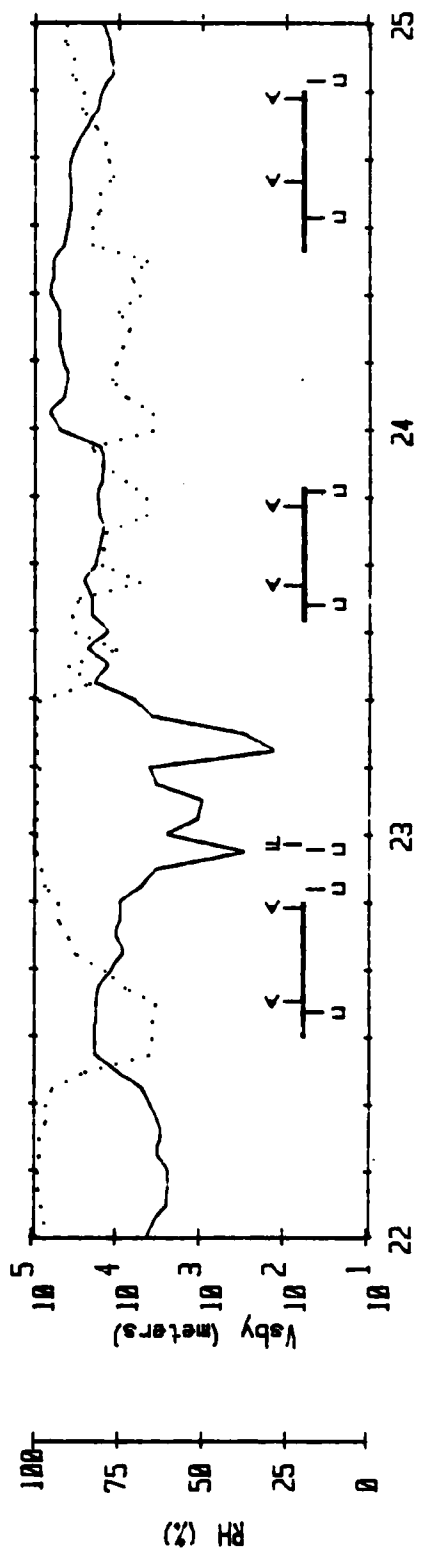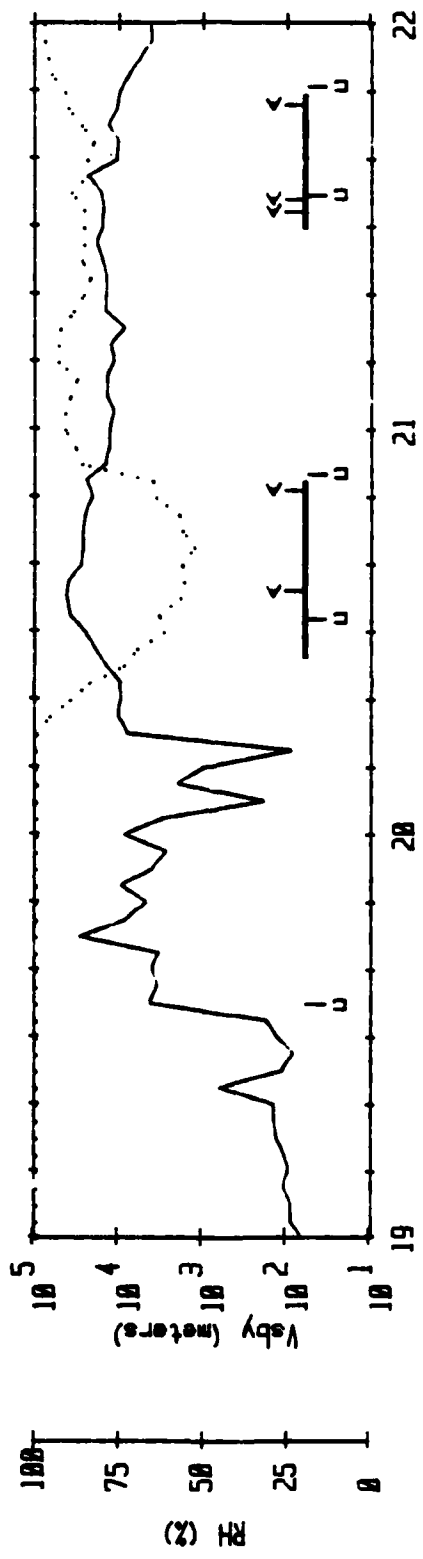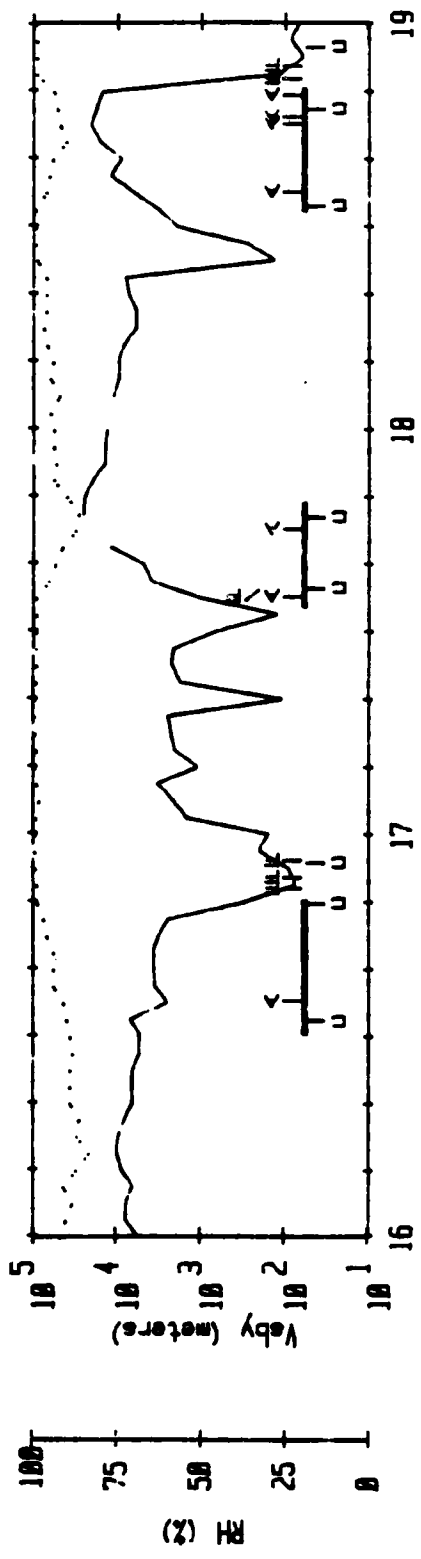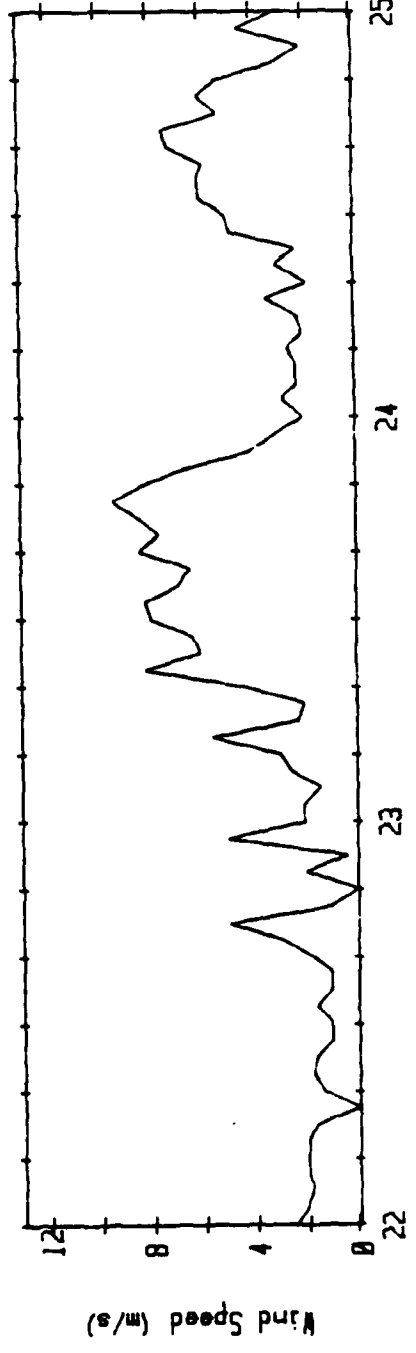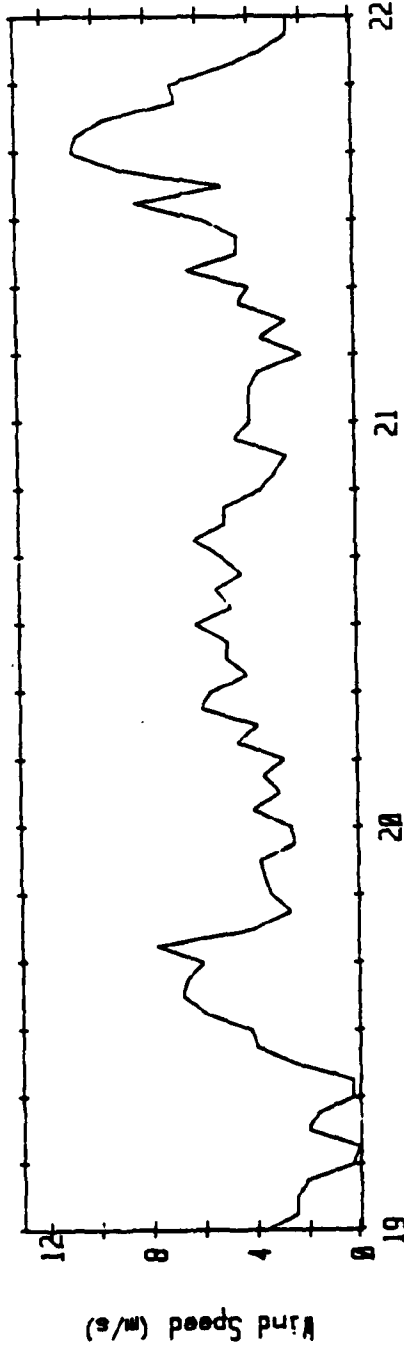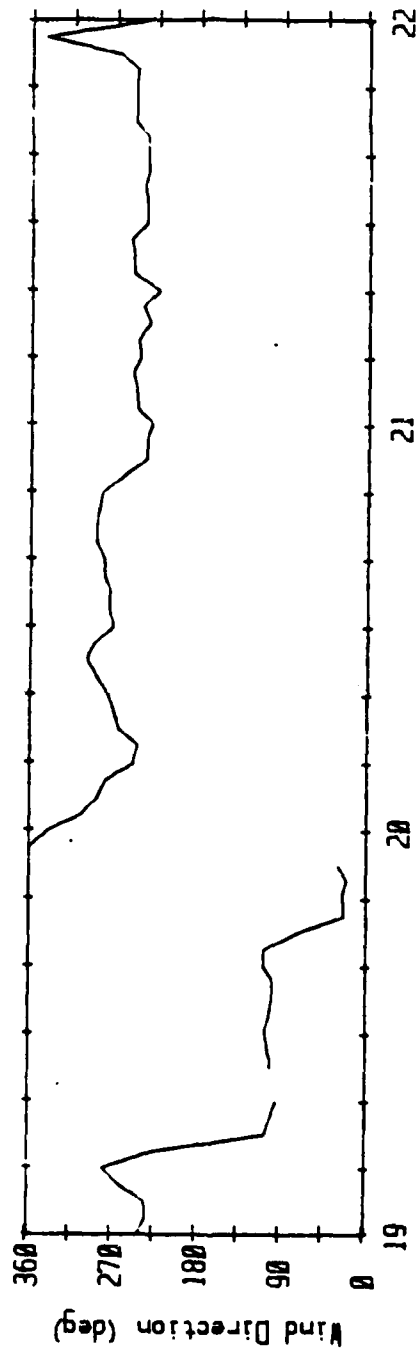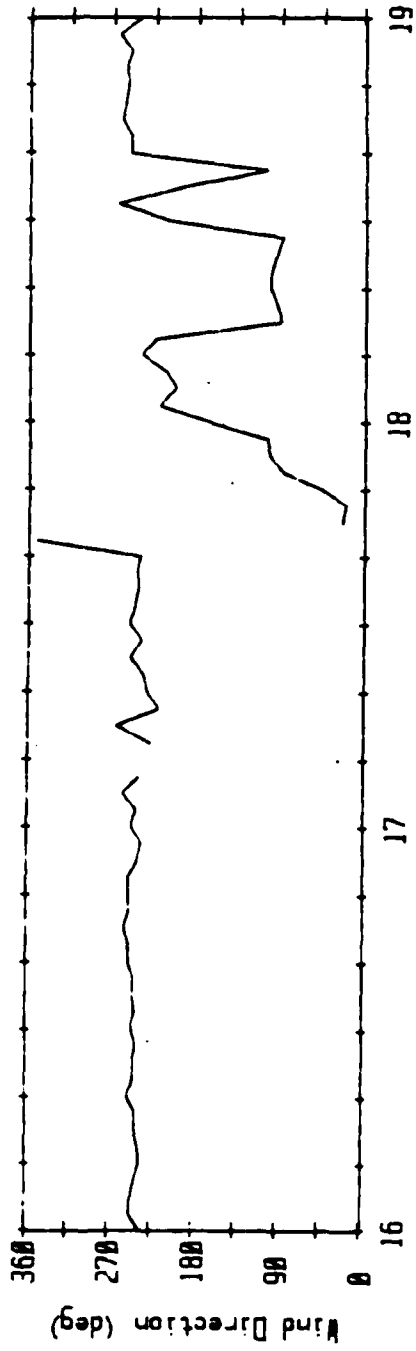
'ocal time)

END

FILMED

02 – 84

DTIC